Bulletin of Engineering Geology and the Environment (2020) 79:5161–5183
https://doi.org/10.1007/s10064-020-01894-9

ORIGINAL PAPER

Assessing channel morphology and prediction of centerline channel migration of the Barak River using geospatial techniques

Wajahat Annayat[1] · **Briti Sundar Sil**[1]

Received: 11 March 2020 / Accepted: 25 June 2020 / Published online: 11 July 2020

Abstract
Barak River is highly meandering rivers flowing through the alluvial plains of Assam in India. However, due to dynamic system, it is found that channel being subjected to regular shifting which creates uncertainty to the habitants residing nearby the river. Therefore, it is anticipated to carry out a study regarding changes in channel morphology and prediction of centerline channel migration during 1984–2030, using multiperiod Landsat remote sensing images along with autoregressive integrated moving average model (ARIMA). From morphometric analysis, it was found that the mean value of meander length (M_L), meander width (M_B), and meander ratio (M_R) indicates an increasing trend, while sinuosity (C), wavelength (λ), and radius of curvature (R_C) show a decreasing trend. The outcome of ARIMA model specifies that channel shifting of mid-line is going to change suddenly either to rightward or leftward directions. Throughout the whole alluvial part of the Barak River, rightward side is recognized as major concern. Observed and predicted values have shown a good R^2 value ($R^2 = 0.89$ and $R^2 = 0.88$) at CS-30 and CS-18 respectively. Also, lowest RMSE is observed at CS-12 and highest RMSE is observed at CS-21. Finally predicted values were generated for the estimation of centerline channel shifting between two time intervals (2017–2023 and 2023–2030), which shows that the channel shifting of the river basin will occur at many regions particularly at critical sections. Overall, the findings of this study could be used further in river training works and in understanding the future dynamics of channel.

Keywords Channel morphology · ARIMA modeling · River meandering · Remote sensing · Barak River

Introduction

In the alluvial plains, common plan shape acquired by rivers is meandering. "The word meandering is derived from the Menderes River, located in southwestern Turkey, and in ancient times known as Maiandros"(da Silva et al. 2017). Natural rivers and their processes are the most significant geomorphic systems which is active on the surface of the earth. An intensive research of meander planform has been carried out all round the world (Fargue 1867; Jefferson 1902; Leopold and Wolman 1957; O'Boyle 1981; Williams 1986; Magdaleno and Fernández-Yuste 2011; Howett 2017). First attempt was made by Fargue (1867), in order to describe the meander planform and suggested that meandering rivers have one mandatory property, namely "the continuity of the change in curvature." Throughout history, meandering rivers have played an essential role in the improvement of human civilization such as water supply, agriculture, inland navigation, and supporting rich aquatic life. Morphology of the rivers is changing over both space and time scales due to erosion of inner bend and deposition of outer bend. The primary source of sedimentation in the river is its own bank erosion (De Rose and Basher 2011). The other sources of sedimentation are adjacent land use, topography, bank soil composition and its shear strength, discharge parameters, and watershed area (Zaimes et al. 2004). Lot of practical challenges has been posed by meandering river because of their dynamic nature (Inglis and Lacey 1947; Jansen et al. 1994; da Silva et al. 2017; Roca et al. 2007). Because of these reasons, meandering has attracted the attention of researchers all around the world

Electronic supplementary material The online version of this article (https://doi.org/10.1007/s10064-020-01894-9) contains supplementary material, which is available to authorized users.

✉ Wajahat Annayat
wajahatannayat123@gmail.com

Briti Sundar Sil
britisil@gmail.com

[1] Department of Civil Engineering, National Institute of Technology, Silchar, Assam 788010, India

for a long time and has assembled a lot of scientific questions requiring an answer. Anthropogenic activities like construction of dams, irrigation, and infrastructural development have a deep impact on the natural flow of the river, thus affecting the sediment transport processes which in turn affects the meandering pattern and dynamic behavior of the river (Wellmeyer et al. 2005). Sometimes these human interferences play more dominant role than the natural forces causing autogenic rivers to lose their dynamic equilibrium, thus leading to overexploitation of natural resources and variation of streamflow (Heitmuller et al. 2017).

Through space and time, the channel migration of river is critical to various geomorphological and river management problems (Milton et al. 1995). Under turbulent conditions of flow, variations occur in the fluid flow and sediment discharge which is associated with the positional change of the river channel known as lateral migration (Yang et al. 1999). Channel shifting is a geomorphological phenomenon that has been of interest to geologist, geomorphologist, and engineers and has been studied in last few years by various researchers (Pati et al. 2008; Tangri 2000; Das et al. 2007). In order to understand the process assigned to river channel shifting, a study has been conducted by Pati et al. (2008) on Majuli island, situated on the middle of river Brahmaputra in Assam. In this study, they observed the trends of erosion in a small part of Majuli island, the area near Kaniajan village in south Majuli—a stretch of about 11 km, using satellite data of 1991, 1997, and 1998. Lawler (1993) has conducted a study on the measurement of river bank erosion and channel shifting using various methods in his study such as sedimentological evidence, botanical evidence, historical sources, planimetric resurvey, repeated cross-profiling, erosion pins, and terrestrial photogrammetry. Fluvial and meandering analysis for the Talar River in Iran has been done using GIS and remote sensing (RS) data (Yousefi et al. 2017). Numerous other studies have investigated the morphological changes of major river basins such as Ganga River in Allahabad, India (Pati et al. 2008); Jamuna River, Bangladesh(Mount et al. 2013); Brahmaputra River, India (Archana et al. 2012); Tammaro River, Italy (Magliulo et al. 2016); Vaitarna and Ulhas Rivers, India (Das and Pardeshi 2018); Pestan River, Serbia (Djekovic et al. 2016); the middle Yangtze River, China (Xia et al. 2016); and Ganges-Padma River system in Bangladesh (Dewan et al. 2017). It has been observed that the Ganga River has changed its course from straight to the braided channel (Dhari et al. 2015). But it is opposite in the case of Yellow River in China, where the river changes from braided to the weak meandering river with decrease in the flow (Yang et al. 1999). The assessment of erosion rate of this river is also done using satellite imagery and remotely sensed data (Chu et al. 2006). Abnormal faults and subsidence position affected the changes in meandering pattern of the Tisza River (Timár 2003). Taking 80 years historical data into account, a study on Ebro River in Spain revealed a 7-km shift in a reach (Ollero 2010). These studies reveal that methods of morphometric analysis and with geospatial techniques are useful in analyzing the dynamics of channel over different time scales. However, comprehensive study of the channel shifting along with the morphometric analysis of the river in the near future period of time in the existing literature has not yet taken into consideration.

Lateral migration creates geomorphic hazards, and predicting and preventing this migration are both difficult and necessary. For prediction of meander migration of a river, several models are available. Majority of these models are based on database of observed data (e.g., Keady and Priest 1977; Nanson and Hickin 1983; Hooke 1980; Brice 1982). However, these equations are limited by the extent of the database and the selection of the parameters for a specific site. As the river system is dynamic and is having random probability distribution which can be analyzed statistically but may not be predicted precisely, various numerical models such as regression model and artificial neural networks are applied in the river system produce results which possess lot of uncertainties (Heo et al. 2009).

In order to understand the problems of river management, an appropriate understanding is needed that how the channel has migrated through definite period of time (Yang et al. 1999). Regardless of that, a lot of research has been done from decades on bank line migration but knowledge on the subject is imperfect, with much work remaining to be done. Different measurement techniques are required for the estimation of bend especially for the places where bank failure is mostly because of extreme flood events and large return periods (Grove et al. 2013). Therefore, studies of channel morphology are essential to evaluate the natural and human influences on morphometric parameters and channel dynamics (Friend and Sinha 1993; Graf 2000).

In Assam, the Barak River flows through alluvial plains and travels almost 102 km in a zigzag manner before entering into Bangladesh. Bank erosion is a regular phenomenon in the alluvial plains of the river, leading to the shifting of its course. Besides, there are several locations on the Barak River where significant bank shifting is observed which can have a devastating effect on the economy and livelihood of the people in near future. Despite all these evident changes in the river channel, no study has been carried out until date to understand the nature and cause of this river migration. In the literature, it is found that no study related to the channel migration has conducted on this river. Therefore, considering the importance of this river and its catchment area, it is intended to carry out a study through which the dynamics of the Barak River can be understood and which will further figure out the actual meandering characteristics of this type of river all over the world. The motivation for the research reported herein is to focus on changes in river morphometric parameters and shifting of centerline channel in order to understand the dynamics of channel of alluvial part of Barak River in the present as well as for future period of time. We try to make an effort on detecting the meandering characteristics and prediction of centerline channel shifting (i.e., 102 km and 33 years) based on Landsat remote sensing images and ARIMA modeling. The detailed aim of the study is outlined as follows:

(i) To analyze the changes in river morphometric parameters in the alluvial part of Barak River.
(ii) To develop a centerline channel shifting river migration prediction model for the Barak River.
(iii) Prediction of centerline channel shifting in the alluvial part of the Barak River from 1984 to 2030.

Outcome of the proposed research will definitely help the government in decision making, management, and implementation of future projects.

Methodology

Study area

The Barak River is the second largest river in the northeastern region in India. The Barak River sources are in the Patkoi hills. The drainage area of the river is 24,220 km^2 up to Badarpur Ghat with a population of 2.98 million. The Barak River starts off from Japvo mountain of Manipur hills at an elevation of 3015 m and follows the course south all the way through hilly terrain up to Tipaimukh close to the tri-junction of the three states: Assam, Manipur, and Mizoram. At this point, the river takes a hairpin curve and enters into the plains of Cachar district of Assam and figures the border of states of Assam and Manipur up to Jirimat, slight upstream of Lakhimpur. Then the river flows through westwards of the Barak valley of Assam. Finally, it enters into Bangladesh where it is known as the Surma River and Kushiyara River. The study area extending from Fulteral Ghat to Badarpur Ghat is located in the state of Assam (Fig. 1). "The Barak basin lies between 89° 50′ E to 94° 0′ E and 22° 44′ N to 25° 58′ N." Bed gradient of Barak River is flat and from upper reach to lower reach, it varies from 1:10,000 to 1:20,000 respectively (Jain et al. 2007). As stated by census of India 2011, the population growth rate is 17.93% in the Barak valley (Deb and Sil 2019). Geological structures like faults, stratigraphic characteristics, and tectonic activity have profound impact on the river morphology. Other factors which affect the bank erosion are geological structures like faults, folds, lineaments, tectonic activity of an area, bed load, and the varied lithology along the river course. Active tectonics can cause steepening or reduction of the river gradient, thus destabilizing the natural equilibrium of the river (Dar et al. 2014). In order to sustain the equilibrium, the river exhibits change in its course, cross-sectional shape, bed and bank erosion, and the meandering pattern (Dar et al. 2014). These changes in the planform geometry of the river are reflected in the variation in channel pattern, channel morphology, degradation, and aggradation (Schumm 1973). Sometimes due to deposition of debris bed load, the river raises its bed, thereby decreasing the depth and increasing the river oscillation leading to bank erosion. Geological and morphotectonic issues of the Barak River can be found in the existing literature of Evans (1932, 1964), Raju (1968), and Seshavataram et al. (1998) during the assessment of hydrocarbons. Fold belt region of Barak River is tectonically surrounded on all four sides. Towards the north side, it is bounded by Dauki. Fault and in the east side, it is bounded by Haflong-Disang Thrust, and on the south side, it is bounded by Arakan-Yoma Fold Belt, while as on the west side, it is enclosed by Hail-Haka-Lulu Lineament and Chandpur-Barisal High (Nandy et al. 1983).

Barak basin has sub-tropical warm and humid climate and receives an annual rainfall of 2500–4000 mm with more than 80% of the annual rainfall occurring from April to October (Choudhury and Ullah 2014). The weather dataset are collected from Cachar meteorological stations which are located within the basin for the period 1911–2012. The mean annual T_{min} and T_{max} ranged from 17.74 to 19.617 °C and 25.147 to 29.652 °C respectively. The vegetative cover along the river bank is thin. The main type of plant communities is bamboo brakes (Bambusoideae), wet as well as dry grasslands (*Phragmites karka*), and savannahs (*Apluda mutica*).

Database

The Landsat images of the Barak River of various years such as 1984, 1992, 2002, 2012, and 2017 are obtained from United States Geological Survey (USGS). Complete information of Landsat images for the present study is shown in Table 1. The Shuttle Radar Topography Mission (SRTM) provides the river network of the Barak River obtained from digital elevation model (DEM), resolution of 30 m which was downloaded from http://earthexplorer.usgs.gov.

Processing of data and analysis

In the present study, five satellite images have been analyzed to investigate the morphological changes in the alluvial part of the Barak River. Morphometric parameters for all of the meander loops for different time periods (1984, 1992, 2002, 2012, and 2017) were measured using different measurement tools in ArcGIS 10.2.2 and AUTOCAD 2012. Bank lines and channel centerlines were digitized and alluvial part of the Barak River was divided into 12 reaches from upstream to downstream within a distance of 102 km for morphometric parameters and morphological changes. River was divided

Fig. 1 Location map of the study area showing Barak River

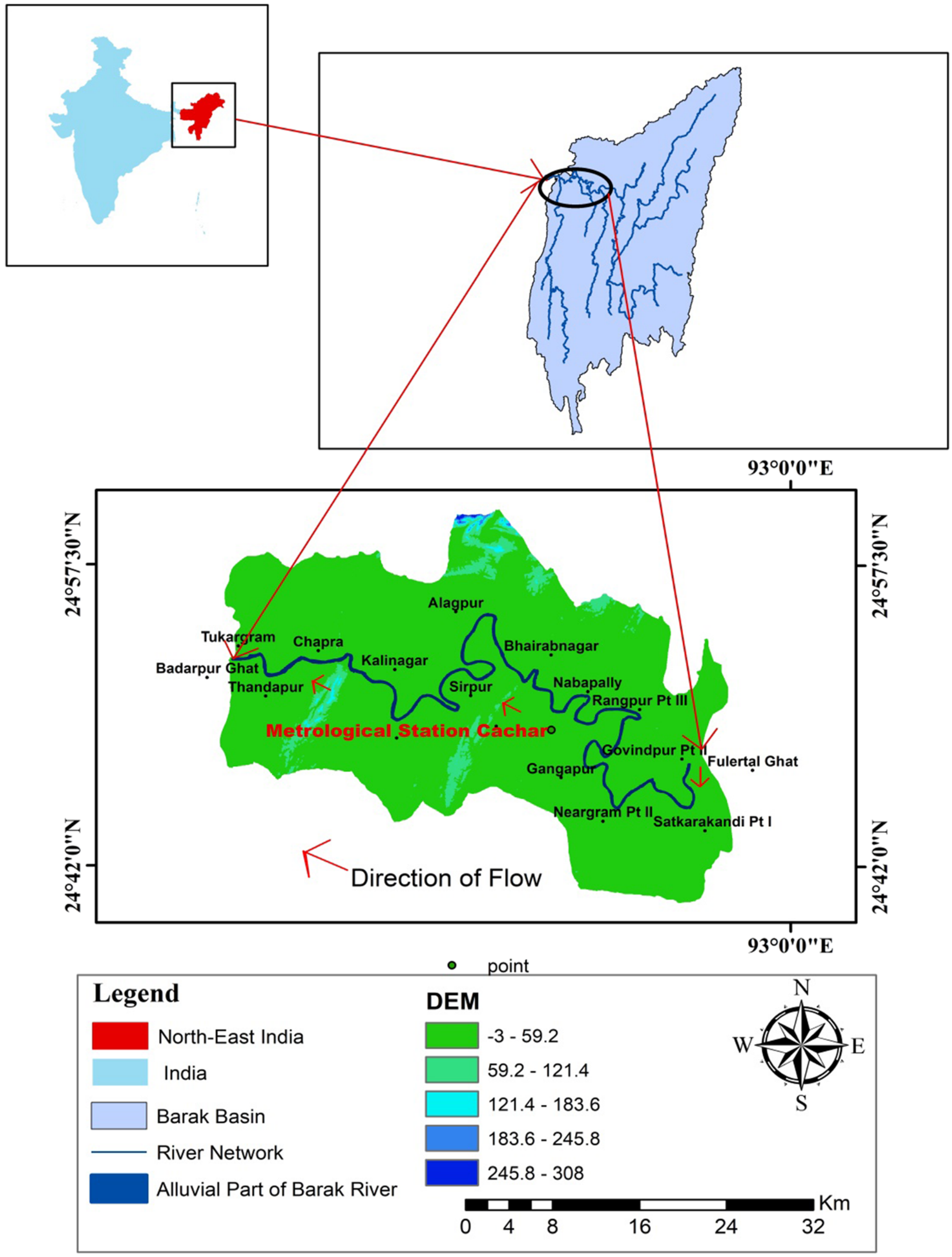

into 41 cross-sections from upstream to downstream which are based on satellite images, e.g., 1984, 1992, 2002, 2012, and 2017, to detect the changes in the width of river. Easy accessibility and freely downloaded are the main reasons to

Table 1 List of Landsat satellite images information

Satellite	Sensor	Path/row	Band used	Resolution	Date (dd/mm/year)	Source
Landsat 1	MSS	136/43	4, 5, 6, 7	60 m	02/01/1984	USGS
Landsat 2	TM	136/43	1, 2, 3, 4	30 m	07/12/1992	USGS
Landsat 5	ETM^{+}	136/43	1, 2, 3, 4	30 m	01/02/2002	USGS
Landsat 7	ETM	136/43	1, 2, 3, 4, 5	30 m	25/02/2012	USGS
Landsat 8	OLI	136/43	1, 2, 3, 4, 5, 6, 7	30 m	20/12/2017	USGS

use Landsat images in the current research. All the available images were downloaded but only clear images were analyzed. Methodology for the measurement of bank line and shifting of mid-channel between different years can be found in the existing literature of Hughes et al. (2006), Thakur et al. (2012), Deb and Ferreira (2015), Jaskuła et al. (2018), and Nawfee et al. (2018). After downloading the Landsat data, it was subjected to line de-stripping as scanning error (line stripping was found), and also the radiometric error and haze corrections were carried out using ERDAS IMAGINE software. Then the MSS data was resampled to 30 m resolution and all the data was georeferenced using various control points which improved positional accuracy. Finally, the data was exported to ARCGIS for the extraction of study area, river, and cross-sections. To study the change in centerline channel migration, a total of 41 cross-sections are considered from upstream to downstream. The sequences of cross-sections are numbered from upstream to downstream. Shifting rates of the river are calculated along all the cross-sections from upstream to downstream during different time periods from the following formulae:

$$r = \frac{y - z}{t} \tag{1}$$

where

- r "shifting rate (m/year)."
- y "intersection point between midline channel and cross-section of the first river."
- z "intersection point between midline channel and cross-section of the river which is compared to the first one."
- t "time difference between the images used in the analysis."

Methodology for the measurement of morphometric parameters such as meander length, meander width, meander ratio, sinuosity, wavelength, radius of curvature, and width can be found in the existing literature of Henshaw et al. (2013), Nicoll and Hickin (2010), and Yousefi et al. (2016). Landsat data have been used for geomorphological analysis by various researchers such as Chu et al. (2006), Peixoto et al. (2009), Ahmed and Fawzi (2011), Thakur et al. (2012), and Henshaw et al. (2013) and have focused on the morphology of channel changes which gives us more confidence to use the Landsat data for the present study. To calculate the sinuosity ratio (SR), the river was divided into twelve reaches starting from upstream to downstream. The formula of sinuosity given by Schumm (1973) is used to calculate the sinuosity ratio which is given below.

$$\mathrm{SR} = \frac{\text{Channel Length}}{\text{Valley Length}} \tag{2}$$

ARIMA modeling

In this study, ARIMA time series model popularized by Box and Jenkins (1970) was employed and is widely used in the applied stochastic time series models (Pourbakhshian and Pouraminian 2015). In order to better understand the data and predict future points in the series, ARIMA model is fitted to time series data. If the series has no trend and is having constant mean and variance, it is said to be stationary series; otherwise, it is considered as non-stationary. As per Box-Jenkins approach, time series modeling is done in four steps: (i) stationarity and normality is checked through differencing and transformation of the series; (ii) estimation of autocorrelation (ACF) and partial autocorrelation function (PACF) to select a tentative model and calculate the amount of linear dependency between observations in a given time series; (iii) use of ACF and PACF to decide whether to include autoregression terms, moving average terms, or both; (iv) build the model and set the number of periods to forecast and compare the predicted values to the actual values in the validation sample. Time series analysis was performed on centerline channel values. In evaluating the performance of ARIMA model, the model that has minimum Bayesian information criterion (BIC) is chosen and validated for centerline channel datasets.

Results and discussion

Changes in river morphometric parameters

During the entire period of the study, Fig. 2 points out that the maximum length of meander was 5496 m at reach-3 (Neairgram part-ii) in 2002 and minimum length of meander was 1643 m at reach-12 (Chapra) in 2002. Mean values of meander length of the Barak River from 1984 to 2017 indicate an increasing trend. A similar range of results has been observed in Manu River of Bangladesh by Mithun et al. (2012) and Bhagirathi River of West Benga by Islam and Guchhait (2017). Figure 3 shows that the maximum width of meander was 3159 m at reach-8 (Bhairabnagar) in 2012 and minimum width of meander was 559 m at reach-1 (Govindapur part-ii) in 1992. Mean values of meander width of the Barak River from 1984 to 2017 indicate an increasing trend. Figure 4 shows that the maximum meander ratio was 1.2 at reach-12 (Chapra) in 2017 and minimum meander ratio was 0.19 at reach-1(Govindapur part-ii) in 1984. Mean values of meander ratio of the Barak River from 1984 to 2017 indicate an increasing trend. Figure 5 shows that the maximum sinuosity was 4.25 at reach-1 (Govindapur part-ii) in 1992 and minimum sinuosity was1.18 at reach-11 (Polarpar) in 1984. In 1984, sinuosity values observed are high (> 1.5) for all the reaches except for reach 11 and reach 12 which indicates the

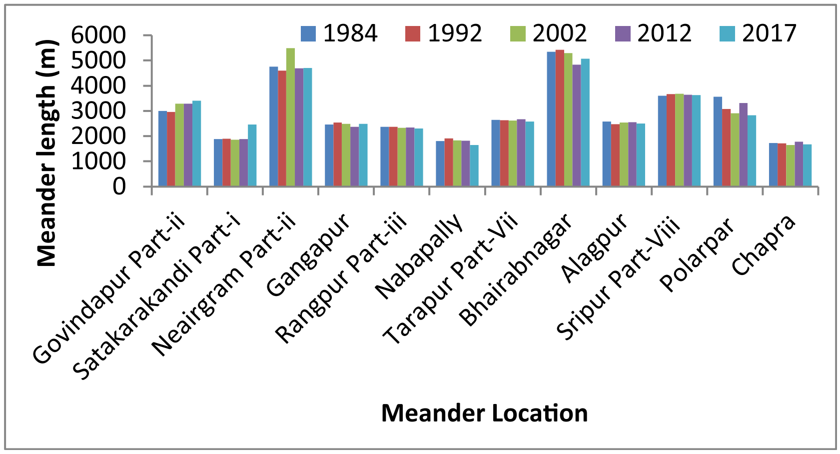

Fig. 2 Variation of meander length with time

meandering nature of the river, although in 2017, there is a slight decrease in the values of sinuosity and river tries to straighten its course. The sinuosity of all the reaches for the year 1984 ranged from 1.18 to 4.25, with a mean and a standard deviation value of 1.85 and 0.738 respectively. Similarly, sinuosity of all the reaches for the year 2017 ranged from 1.23 to 2.48, with a mean and a standard deviation value of 0.754 and 0.45 respectively. During 1984 at reach-1, Barak River was flowing through the highly meandering channel with the sinuosity of 4.25, but after that period, it started to straighten its course through releasing meander necks/cutoffs, migrated inwards, prolonged with a great deformation in shape, leading to the formation of an oxbow lake. Neck cutoff and re-development have also been observed at reach-3, and also apex of reach-3 is deflecting inwards, with migration rate of 33.07 m/year from 1984 to 2017. At this rate and continued pathway migration, the possibility of cutoff formation is high in near future. The sinuosity of the Barak River at various locations decreased from 1984 to 2017. This decrease is mainly attributed to the cutoff in the two meanders at the upstream location, although for most of the reaches, sinuosity was more than 1.5 and the river was meandering. Mean values of sinuosity of the Barak River from 1984 to 2017 indicate a decreasing trend. Leopold and Wolman (1957) suggested that if the value of sinuosity is greater than 1.5, channel is considered to be a meandering channel. The overall high sinuosity values of the studied river are comparable with the results reported by Debnath et al. (2017) (S.R ~ 1.75–2.30), Bag et al. (2019) (S.R ~ 1.70–2.14), and Mithun et al. (2012) (S.R ~ 2.39–2.48). Figure 6 shows that the maximum wavelength of meander was 7637 m at reach-12 (Chapra) in 1984 and minimum wavelength of meander was 918 m at reach-1 (Govindapur part-ii) in 1984. Mean values of meander wavelength of the Barak River from 1984 to 2017 indicate a decreasing trend. Figure 7 shows that the maximum radius of curvature of meander was 1238.27 m at reach-3 (Neairgram part-ii) in 2002 and minimum radius of curvature of meander was 329 m at reach-6 (Nabapally) in 2017. Mean values of radius of curvature of the Barak River from 1984 to 2017 indicate a decreasing trend. Channel wavelength and radius of curvature alone are not able to reveal any qualitative or quantitate measure of meander intensity. However, there is a direct relationship between wavelength and width (Zolezzi et al. 2012). Channel wavelength to channel width (λ/w) ratio of the studied river that ranges between 5.53 and 12.9 is comparable with the results reported by Nanson and Hickin

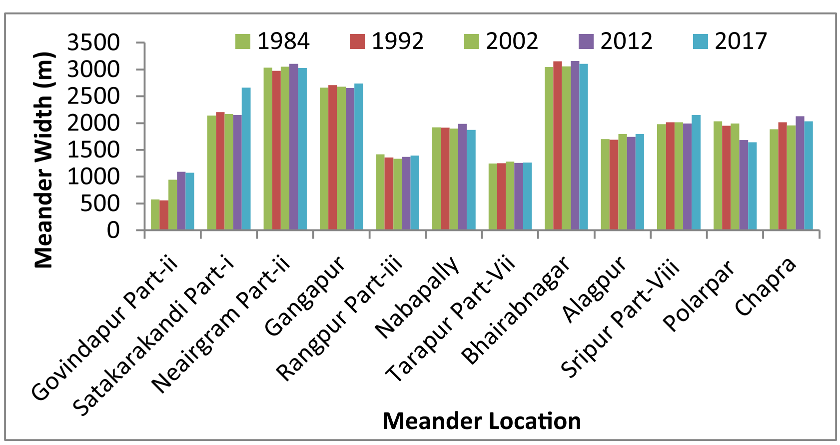

Fig. 3 Variation of meander width with time

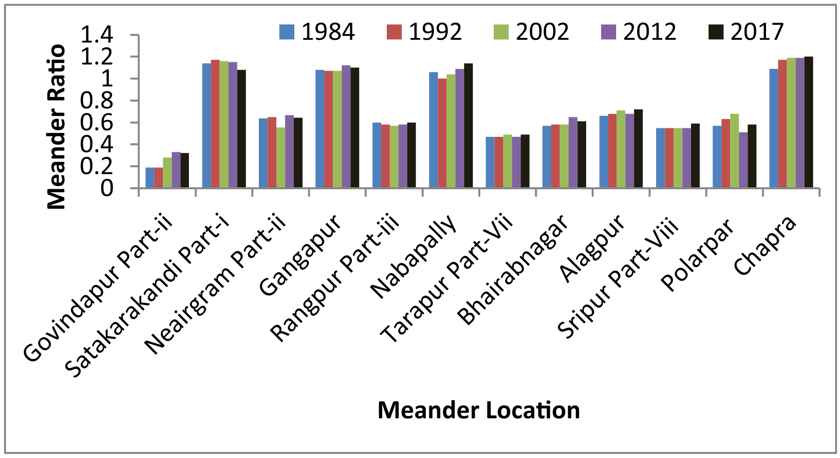

Fig. 4 Variation of meander ratio with time

(1986) ($\lambda/w \sim 8$–14). Radius of curvature to channel width (R_C/w) ratio of the studied river that ranges between 1.1 and 3.93 is comparable with the results reported by Nanson and Hickin (1986) ($R_C/w \sim 2$–3). Meandering is the natural geomorphic feature in rivers which leads to regular migration of river course and erosion of banks (Akhter et al. 2019). Meandering tendency of Barak River at reach-1 has been reduced than earlier times. A result of the meander morphology shows that the simple and double type of meander changes has occurred through time in the meander reaches of the Barak River. From Fig. 8, various meander reaches such as 2, 7, 8, 9, 10, and 11 signify double type of changes. Reach-2 migrated by extension and rotation, reach-7 by rotation and extension, reach-8 by translation and rotation, reach-9 and reach 10 by rotation and translation, and reach-11 by extension and rotation processes. From the analysis, it was observed that the Barak River within the study reach is predominantly irregular channel. It was found that the reaches of the Barak River were migrating inward or outward from the period during 1984–2017. Also all types of bend migration were observed to occur (extension, rotation, and translation). The overall meander morphological changes of the studied river are comparable with the results reported by Mithun et al. (2012) (extension, rotation, and translation) and Yousefi et al. (2016) (translation, rotation, extension, cutoff, redevelopment, lateral movement, and irregular change). A t test conducted at 5% confidence level shows considerable difference between M_R and W (Table 2). However, no significant difference was observed for M_L, M_B, C, λ, and R_C between 1984 and 2017.

Changes in river width

Table S1 shows that from period of 1984–2017, changes in the river channel width varied reasonably. From 1984 to 1992, the highest change in width was observed at CS-21 and CS-23 where it was increased by 323.41 and 327.64 m respectively (Fig. 9a). In contrast, the width of river decreased by 152.82 m at CS-16. Decrease in width was observed from 1992 to 2002 at various cross-sections such as at CS-6 by 93.39 m in Satkarakandi part-1, CS-24 by 217.89 m in Alagpur, and CS-41 by 93.39 m in Tukargram (Fig. 9b). In 2002–2012, the width of the river was increased at CS-6 by 189.5 m, CS-24 by 185.57 m, CS-40 by 128 m, and CS-41 by 114.8 m. However, CS-23 and CS-36 showed a decrease in width by 85.91 and 66.06 m respectively (Fig. 10a). Furthermore, from 2012 to 2017, CS-2, CS-6, CS-10, CS-21, CS-25, CS-26, and

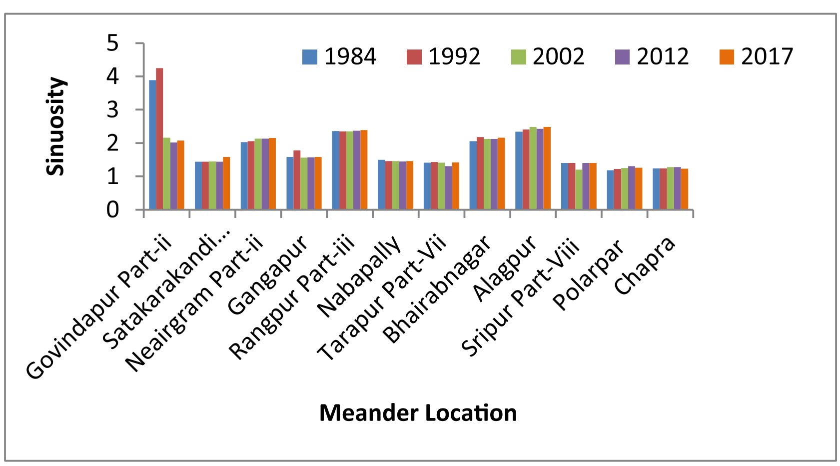

Fig. 5 Variation of changes in sinuosity with time

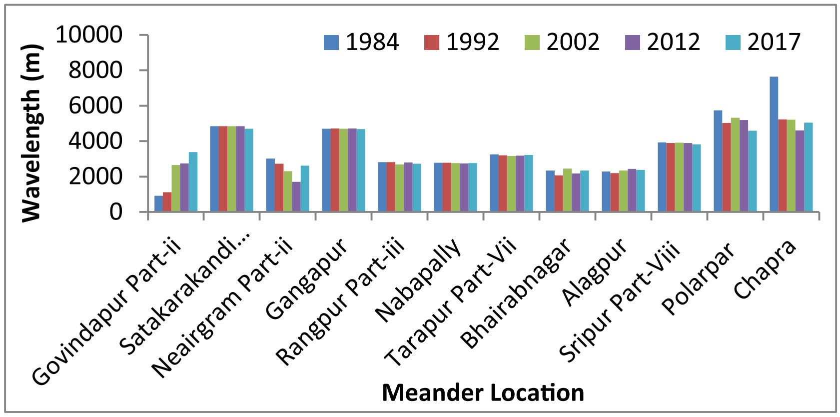

Fig. 6 Variation of meander wavelength with time

CS-41 showed a decrease in width. However, CS-5, CS-11, CS-16, CS-19, and CS36 showed an increase in width (Fig. 10b). From the period of 1984–2017, CS-36 showed an increase in width by 249.93 m and CS-25 showed a decrease in width by 18.83 m (Fig. 11). From various time periods, river channel width shows contraction and expansion. Figure 12 shows spatiotemporal changes in the river width during the study period. Average increase in width was found to be 104.11 m and average decrease in width was found to be 13.18 m. Also maximum width identified along CS-21 was 595.36 m in 1992 and minimum width identified along CS-15 was 208.81 m in 1984. It can be said that the overall width of Barak River has been expanded from 1984 to 2017. Increase in width has occurred due to following reasons. First, the morphology of the river has been changed from time being. Second, erosion and flow of river water are the main factors of the channel change. Debnath et al. (2017) suggested that an increase in the trend of width along the river reach indicates predominantly high lateral erosion. The width change given in Table S1 indicates that the width of the Barak River has been increasing from 1984 to 2017 eroding a large portion of land along both sides of the river bank. Third, morphometric parameters might be responsible for the change in the river width. Nanson and Hickin (1983) and Nanson and Hickin (1986) suggested that if the ratio of radius of curvature to width (R_C/W) is between 2 and 3, the rate of lateral erosion is high. The ratio of radius of curvature to width calculated in this study was found between 1.1 and 3.93. This showed that the Barak River has high rate of lateral bank erosion. Das (2018) in the study of Pravara basin, India, found that morphometric parameters are accountable for the change in channel morphology. Third, the basin undergoes sub-tropical warm and humid climate and average annual rainfall recorded is 2940.78 mm. Both velocity and discharge get accelerated due to intense rainfall which finally results in an increase in various parameters such as river becomes deeper and wider and flows at higher velocity. Debnath et al. (2017) in a study of Khowai River reported that intense rainfall (1873.6 mm annually) induces bank erosion which is similar to our study. According to CWC data, mean annual daily discharge at the outflow gauging station (Badarpur Ghat) from 2000 to 2015 of the Barak River is 322,832.2 m^3/s and maximum annual discharge is 532,465.4 m^3/s. When a stream channel can no longer accommodate increased discharge, it

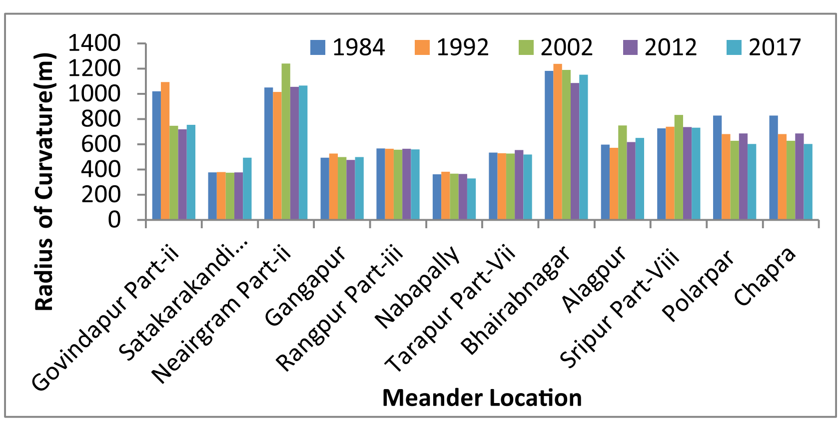

Fig. 7 Variation of radius of curvature with time

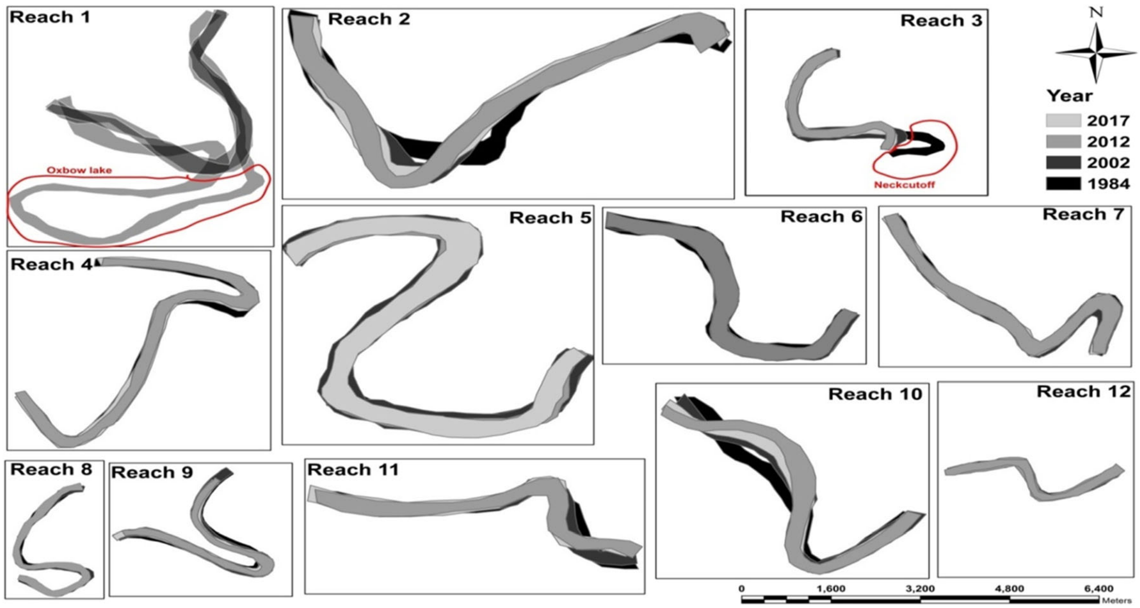

Fig. 8 Meander reaches of the Barak River showing morphological change

overflows its banks and high amplitude of flood occurs which is likely to induce intense bank erosion in short period.

Time-based lateral shifting of centerline channel

Centerline channel shifting for the year 1984, 1992, 2002, 2012, and 2017 are shown in Table 3. Shifting of centerline was measured between two selected years. Here shifting of centerline was calculated with a base image for the year 1984–2002, 1884–1992, 1984–2012, and 1984–2017 with 41 CS. Shifting of centerline has either occurred in the rightward direction or leftward direction. During 1984–1992 time intervals among 41 CS, 34 CS reveal rightward movement and 7 CS reveal leftward movement. Due to high rate of lateral shifting from 1984 to 1992, it clearly shows that erosion of bank has occurred in the right bank. Also maximum centerline shifting (2378.23 m) was observed at CS-6 under Satkarakandi part-1, whereas minimum centerline shifting (16.25 m) was found at CS-41 under Tukargram (Table 3). During 1984–2002, maximum centerline shifting (2344.73 m) was observed at CS-6 under Satkarakandi part-1, whereas minimum centerline shifting (11.23 m) was found at CS-12 (Table 3). In 1984–2012 time interval, the highest shifting (2850.67 m) occurred along CS-6 in the right side in the Satkarakandi part-1 whereas the lowest shifting (9.05 m) occurred along CS-20 in the left side near Tarapur part-vii (Table 3). During 1984–2017, maximum centerline shifting (2828.98 m) was observed at CS-6 under Satkarakandi part-1 whereas minimum centerline shifting (5.97) was found at CS-12 (Table 3).

Centerline channel shifting prediction

In order to recognize the future trend of shifting channel of alluvial part of Barak River, channel movement of centerline is determined first and then the future predictions for the two time periods, i.e., 2017–2023 and 2024–2030 using ARIMA modeling. All the observed and predicted values of the centerline channel shifting from CS-1 to CS-41 are shown in

Table 2 Results of sample *t* test for the parameters of meanders between 1984 and 2017

Meander parameters	Average difference between variables	Standard deviation	Sample size (*N*)	Degrees of freedom	*T* value	*P* value
M_L	− 0.015	0.347	12	11	− 0.158	0.439
M_B	− 0.094	0.2446	12	11	− 1.334	0.1046
M_R	− 0.043	0.0507	12	11	− 2.906	0.007*
C	0.0917	0.5192	12	11	0.612	0.723
λ	0.182	1.1356	12	11	0.554	0.295
R_C	0.051	0.1185	12	11	1.486	0.917
W	− 0.080	0.0466	12	11	− 6.008	0.0004*

*Significance at 5% confidence level

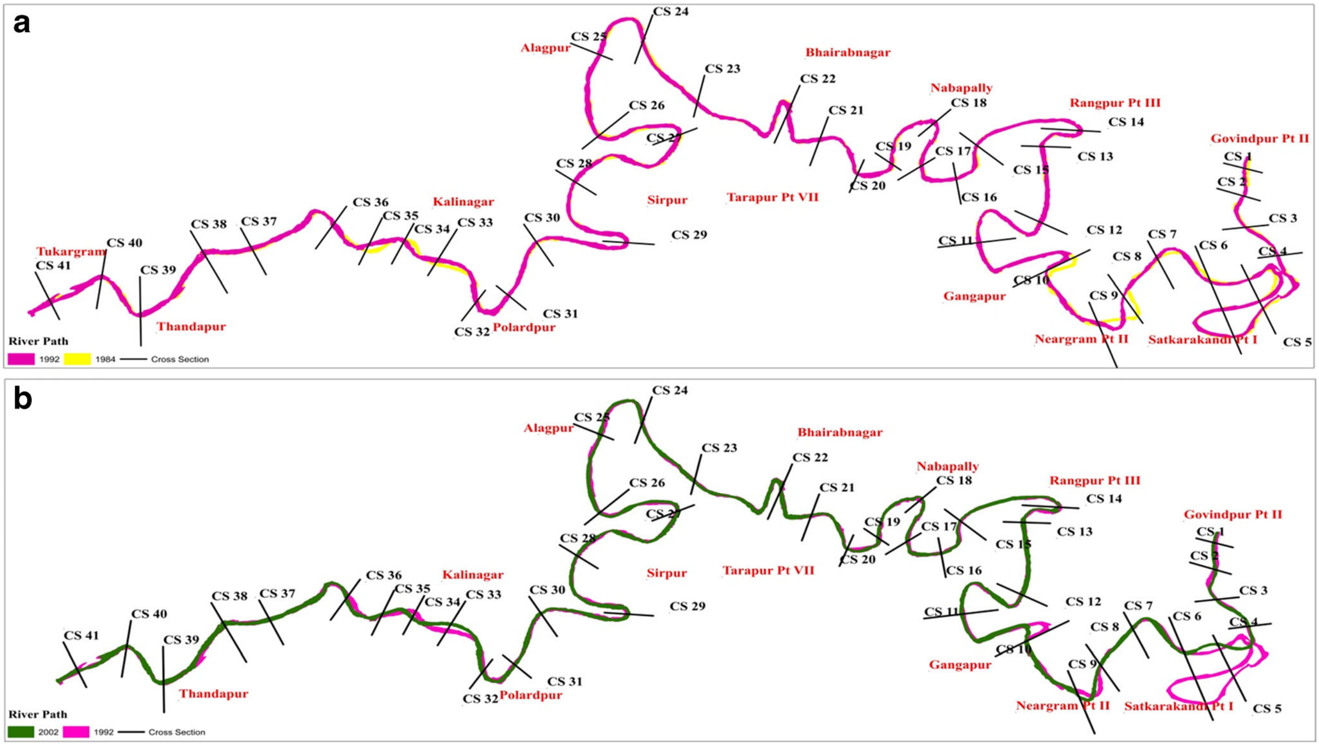

Fig. 9 Spatiotemporal changes of the Barak River width and shifting direction from **a** 1984–1992 and **b** 1992–2002

Fig. 13. From the analysis, it is witnessed that the centerline channel shifting will change suddenly either to rightward or leftward directions and among all the CS, right side of the river is recognized as the core concern. Every CS was evaluated on the basis of coefficient of determination (R^2), root mean square error (RMSE), and Bayesian information criteria (BIC) to assess the accuracy. Observed and predicted values have shown good R^2 values ($R^2 = 0.89$ and $R^2 = 0.88$) at CS-30 and CS-18 respectively. Also, the lowest RMSE is observed at CS-12 and the highest RMSE is observed at CS-21 (Table 3) and finally predicted values were generated for the estimation of centerline channel shifting between two time

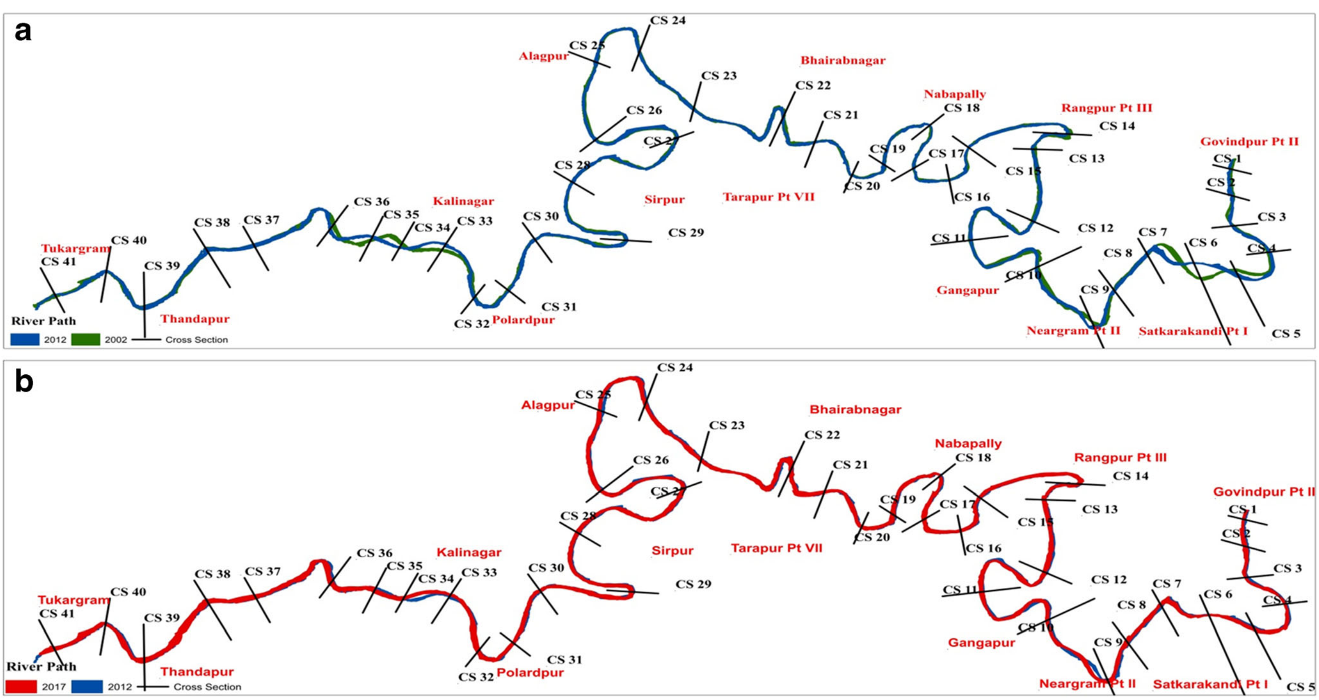

Fig. 10 Spatiotemporal changes of the Barak River width and shifting direction from **a** 2002–2012 and **b** 2012–2017

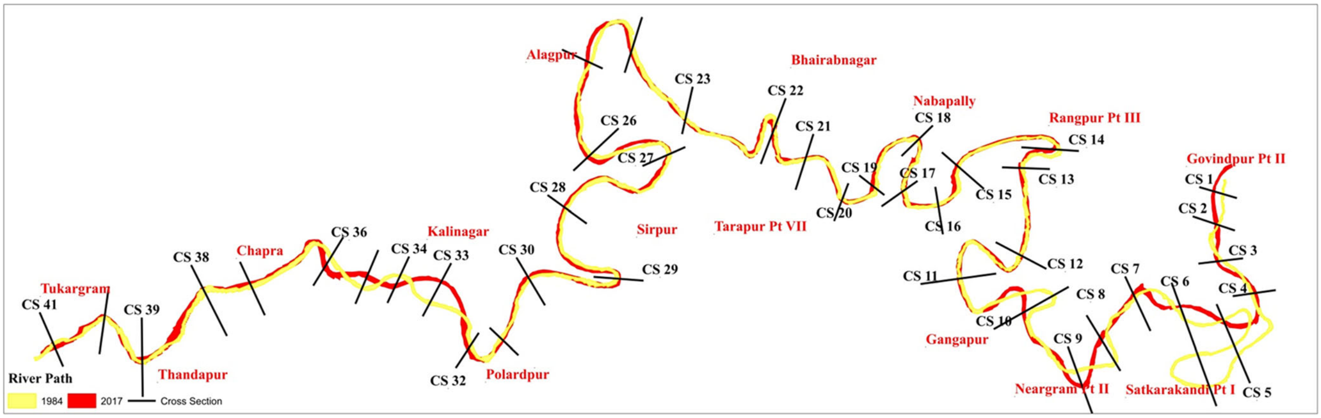

Fig. 11 Spatiotemporal changes of the Barak River width and shifting direction from 1984 to 2017

intervals (2017–2023 and 2023–2030), which shows that the channel shifting of the river basin will occur at many regions particularly at critical sections (CS-5, CS-6, CS-9, CS-10, CS-33, CS-34, CS-35, and CS-36). Timár (2003), Ollero (2010), and Engel and Rhoads (2012) suggested that riparian vegetation cover is important factor for the process of river migration that controls bank erosion. Along the alluvial plains of the Barak River, thin riparian vegetative cover, fine-grained non-cohesive sediments (fine sand), and displaced floodplains may explain the reason behind the centerline channel shifting in the critical regions of the river basin. In the study of Nile River reported by Ahmed and Fawzi (2011), they found that erosion of banks is more in agricultural lands than in riparian vegetation lands. Hence, it can be said that vegetative cover plays an important role for the process of centerline channel shifting. Li et al. (2017) in a study of Tarim River, northwestern China, reported that fine-grained non-cohesive sediments have limited resistance to erosion. Therefore, the presence of loose bed and bank materials is prone to excessive erosion due to limited resistance and thus leads to amplified lateral erosion of the banks. Findings of the present study will help us to understand the future channel dynamics of the alluvial part of the Barak River and also it will be beneficial to the habitants residing nearby the river so that in the near future if any physical hazard will occur, they will make their sustainable plan for their livelihood. In the near future period (2017–2023), maximum rightward shift will occur at CS-6 (2898.38 m) and maximum rightward shift will occur at CS-6 (2968.23 m) that will happen during 2023–2030 (Table 3).

Prediction of centerline channel migration given in Table 3 shows that in future period 2017–2023, maximum centerline channel migration is expected in the rightward direction with maximum migration at CS-6 in Satkarakandi part-1 (2898.38 m) and minimum migration at cross-section-22 in Bhairabnagar (20.36 m). On the other hand from period 2023–2030, maximum migration is at CS-6 in Satkarakandi part-1 (2968.23 m/year) and minimum migration is at CS-21 near Tarapur part-vii (0.33 m/year). Also in time period of 2023–2030, same rate of centerline channel shifting (40.52 m) will occur in leftward direction at CS-26 near Sirpur and rightward direction at CS-40 near Tukargram. Results obtained from the ARIMA model showed that throughout the whole reach of the river, among 41 CS, centerline channel shifting on the rightward side is noticed as main concern. We propose that the outcomes will help in recognizing the future hazards in the areas of the centerline channel and these effects may be prevented by efficient planning of settlements and to adopt some bank protection measures.

Fig. 12 Spatiotemporal changes of river width at cross-sections 1–41 in the study area

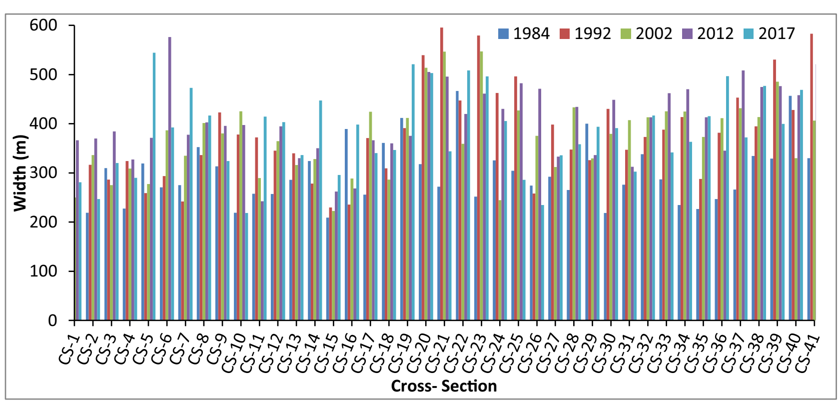

Table 3 The assessment of mid-line channel shifting and prediction of mid-line channel using the ARIMA model. *R.B* right bank, *L.B* left bank

Cross-section	1984–1992	1984–2002	1984–2012	1984–2017	2017–2023	2023–2030	RMSE	R^2	BIC
CS-1	178.45 (R.B)	160.25 (R.B)	160.53 (R.B)	190.24 (R.B)	229.699 (R.B)	287.23 (R.B)	6.08	0.75	3.93
CS-2	165.29 (L.B)	163.03 (R.B)	145.26 (R.B)	157.13 (R.B)	145.37 (L.B)	129.479 (L.B)	8.96	0.30	4.71
CS-3	146 (R.B)	175.45 (L.B)	100.88 (L.B)	82.9 (L.B)	67.71 (L.B)	50.61 (L.B)	14.18	0.82	5.62
CS-4	122.30 (R.B)	117.64 (R.B)	130.29 (L.B)	125.22 (L.B)	128.87 (R.B)	130.38 (R.B)	7.54	0.38	4.46
CS-5	1600.37 (R.B)	1582.31 (L.B)	1490.02 (R.B)	1480.83 (R.B)	1476.92 (L.B)	1451.43 (L.B)	19.81	0.84	6.39
CS-6	2378.23 (R.B)	2344.73 (L.B)	2850.67 (R.B)	2828.98 (R.B)	2898.38 (R.B)	2968.23 (R.B)	82.39	0.85	9.14
CS-7	186.88 (R.B)	192.91 (R.B)	246.16 (R.B)	268.68 (R.B)	280.97 (R.B)	296.18 (R.B)	5.58	0.81	3.84
CS-8	19.6 (R.B)	22.93 (L.B)	45.6 (L.B)	58.12 (L.B)	65.75 (R.B)	73.04 (R.B)	4.39	0.71	3.38
CS-9	240.5 (L.B)	148.66 (L.B)	507.08 (L.B)	540.75 (L.B)	579.25 (R.B)	626.16 (R.B)	62.29	0.82	8.58
CS-10	1062 (R.B)	1048.22 (L.B)	1076.31 (L.B)	1092.52 (L.B)	1096.72 (R.B)	1104.76 (R.B)	6.20	0.73	3.83
CS-11	18 (R.B)	14.39 (R.B)	34.6 (L.B)	26.35 (L.B)	25.46 (L.B)	27.09 (R.B)	2.94	0.76	2.37
CS-12	17 (R.B)	11.23 (R.B)	9.59 (R.B)	5.97 (L.B)	6.10 (L.B)	4.56 (L.B)	2.22	0.60	1.81
CS-13	25 (R.B)	12.39 (R.B)	35.16 (L.B)	45.45 (R.B)	49.13 (R.B)	54.05 (R.B)	3.68	0.85	2.82
CS-14	265.1 (R.B)	209.95 (R.B)	320.18 (R.B)	275.96 (R.B)	245.07 (L.B)	232.06 (L.B)	13.78	0.83	5.45
CS-15	43 (R.B)	48.79 (R.B)	35.2 (R.B)	54.67 (R.B)	78.75 (R.B)	111.54 (R.B)	3.76	0.74	2.97
CS-16	34 (R.B)	19.26 (L.B)	57.24 (R.B)	61.83 (L.B)	69.80 (R.B)	79.86 (R.B)	4.14	0.81	3.16
CS-17	21 (L.B)	17.7 (R.B)	20 (L.B)	8.78 (L.B)	4.01 (L.B)	22.6 (L.B)	3.83	0.66	3.01
CS-18	24 (L.B)	15.67 (R.B)	36.5 (R.B)	63.97 (R.B)	96.39 (R.B)	140.27 (R.B)	4.24	0.88	3.21
CS-19	156.23 (R.B)	128.43 (R.B)	185.69 (R.B)	191.32 (R.B)	185.63 (L.B)	176.49 (L.B)	11.70	0.71	5.24
CS-20	26.23 (R.B)	22.67 (R.B)	9.05 (L.B)	13.99 (L.B)	17.64 (R.B)	20.54 (R.B)	2.82	0.87	2.40
CS-21	26 (R.B)	29.84 (R.B)	16.66 (R.B)	18.06 (L.B)	10.38 (L.B)	0.33 (L.B)	2.54	0.81	2.19
CS-22	140.32 (R.B)	86.64 (L.B)	80.54 (L.B)	30.39 (L.B)	2.36 (L.B)	31.6 (R.B)	10.05	0.73	4.93
CS-23	71.23 (R.B)	69.81 (L.B)	70.89 (L.B)	51.71 (L.B)	44.47 (L.B)	38.17 (L.B)	6.10	0.76	3.93
CS-24	85.21 (R.B)	77.71 (L.B)	110.5 (L.B)	94.95 (L.B)	95.24 (R.B)	97.37 (R.B)	15.15	0.61	5.76
CS-25	85.8 (R.B)	61.4 (L.B)	95.25 (L.B)	76.08 (L.B)	79.13 (R.B)	78.56 (R.B)	11.38	0.30	5.40
CS-26	92.3 (L.B)	75.8 (L.B)	65.74 (L.B)	94.04 (L.B)	72.63 (L.B)	40.52 (L.B)	8.41	0.58	4.58
CS-27	47.3 (R.B)	43.71 (L.B)	84.08 (L.B)	85.86 (L.B)	106.47 (R.B)	136.66 (R.B)	4.81	0.82	3.46
CS-28	33.5 (R.B)	25.34 (R.B)	19.95 (L.B)	21.39 (L.B)	20.44 (L.B)	19.03 (L.B)	4.33	0.49	3.25
CS-29	31.36 (R.B)	33.55 (L.B)	68.12 (L.B)	84.17 (L.B)	103.04 (R.B)	127.33 (R.B)	4.40	0.74	3.29
CS-30	49.56 (R.B)	35.87 (R.B)	75.63 (R.B)	96.98 (R.B)	128.01 (R.B)	173.45 (R.B)	6.08	0.89	3.93
CS-31	60.25 (R.B)	48.89 (L.B)	145.45 (L.B)	123.97 (L.B)	126.95 (R.B)	130.96 (R.B)	11.48	0.80	5.19
CS-32	78.56 (R.B)	48.29 (L.B)	154.7 (L.B)	129.55 (L.B)	134.66 (R.B)	143.54 (R.B)	13.10	0.80	5.44
CS-33	380.25 (L.B)	400 (R.B)	500.36 (R.B)	666.62 (R.B)	835.08 (R.B)	1074.23 (R.B)	19.32	0.71	6.25
CS-34	265.85 (R.B)	325.62 (L.B)	346.59 (L.B)	387.25 (L.B)	465.74 (R.B)	584.70 (R.B)	29.30	0.55	7.08
CS-35	269.65 (R.B)	281.88 (R.B)	405.55 (R.B)	422.17 (R.B)	471.80 (R.B)	536.86 (R.B)	8.33	0.78	4.56
CS-36	265.65 (R.B)	219.39 (L.B)	369.61 (L.B)	416.2 (L.B)	508.92 (R.B)	643.86 (R.B)	13.99	0.74	5.60
CS-37	72.52 (R.B)	58.64 (L.B)	66.41 (L.B)	76.27 (L.B)	80.60 (R.B)	85.96 (R.B)	3.76	0.55	2.96
CS-38	42.5 (R.B)	16.09 (R.B)	48.05 (R.B)	30.24 (R.B)	14.03 (R.B)	5.59 (L.B)	4.97	0.76	3.53
CS-39	152.74 (R.B)	107.64 (R.B)	79.95 (R.B)	89.9 (R.B)	69.11 (L.B)	47.51 (L.B)	5.55	0.87	3.74
CS-40	70.54 (L.B)	66.81 (R.B)	58.78 (R.B)	53.45 (R.B)	40.44 (L.B)	20.63 (L.B)	5.48	0.63	3.72
CS-41	16.25 (R.B)	15.77 (R.B)	16.7 (L.B)	40.03 (L.B)	40.06 (R.B)	40.52 (R.B)	3.83	0.77	3.04

Shifting rates of the Barak River

Table 4 shows the shifting rates of the Barak River which are found from CS-1 to CS-41. In the right bank side, shifting rates are changed from 0.34 to 297.27 m/year and 0.180 to 130.263 m/year in the left side of the bank. During 1984–1992, the highest centerline shifting rate was found at the rightward direction at CS-6 in Satkarakandi part-1. During 1984–2002, maximum

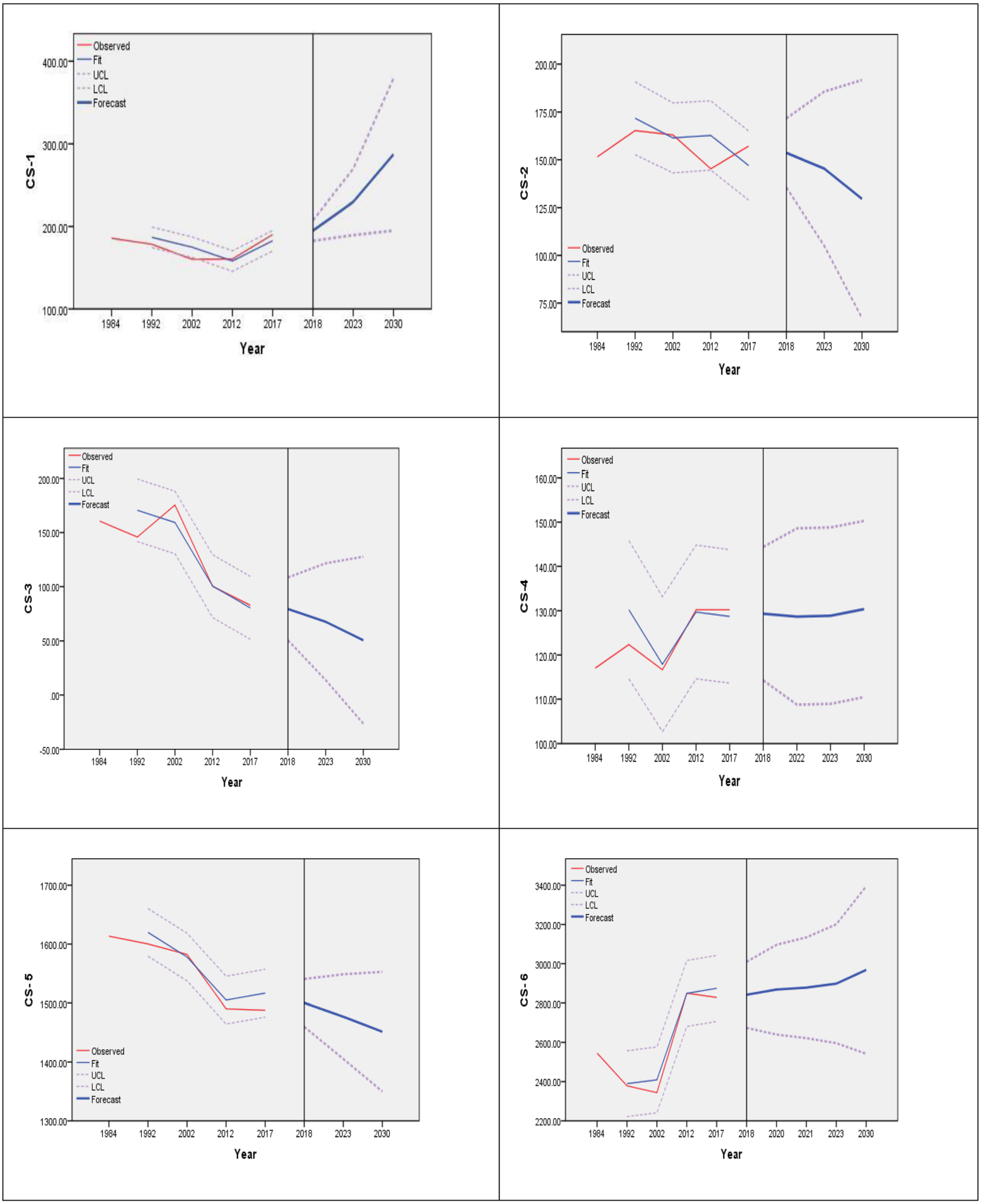

Fig. 13 Prediction for the centerline channel of the river in 2017–2023 and 2023–2030 time intervals using ARIMA model

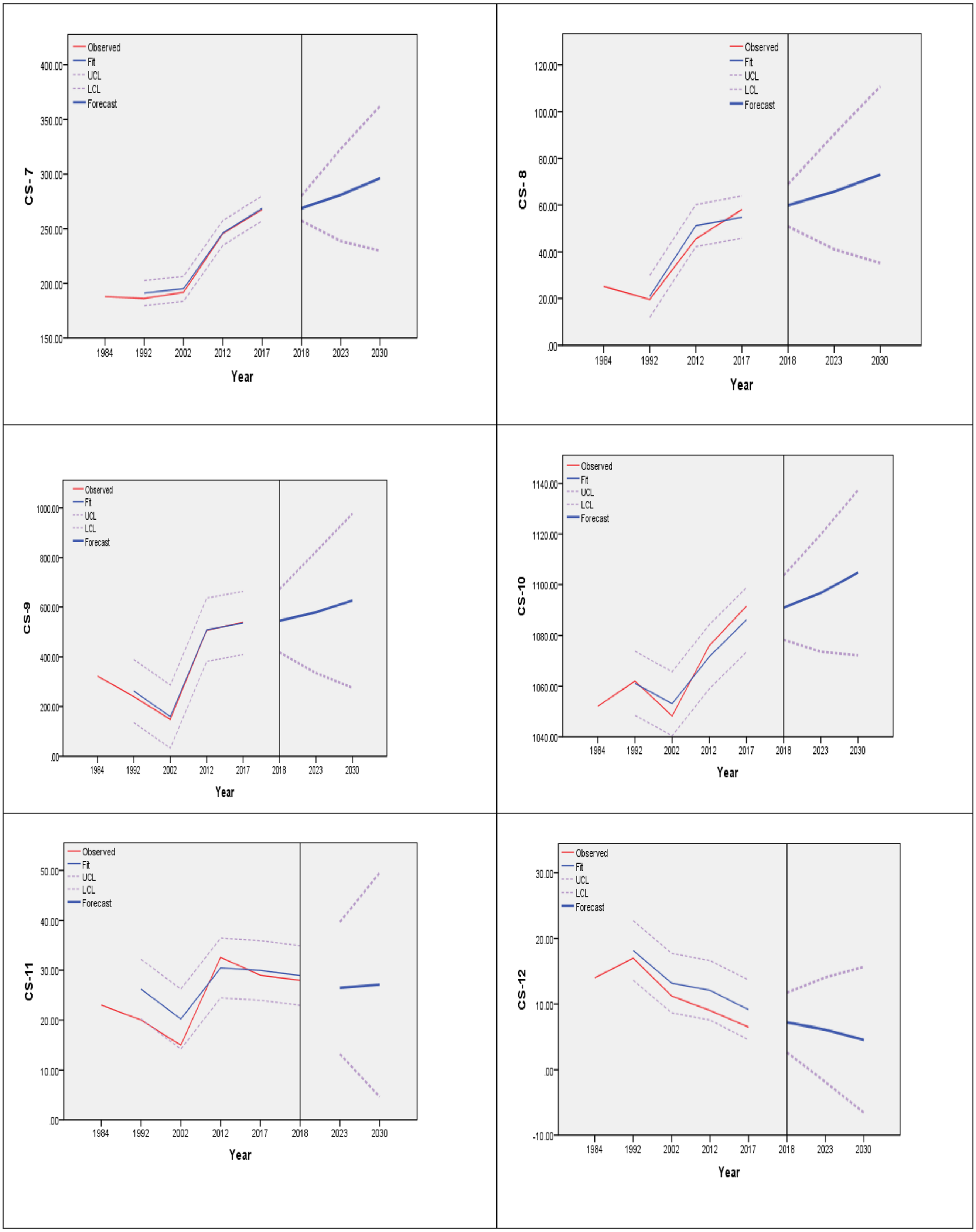

Fig. 13 continued.

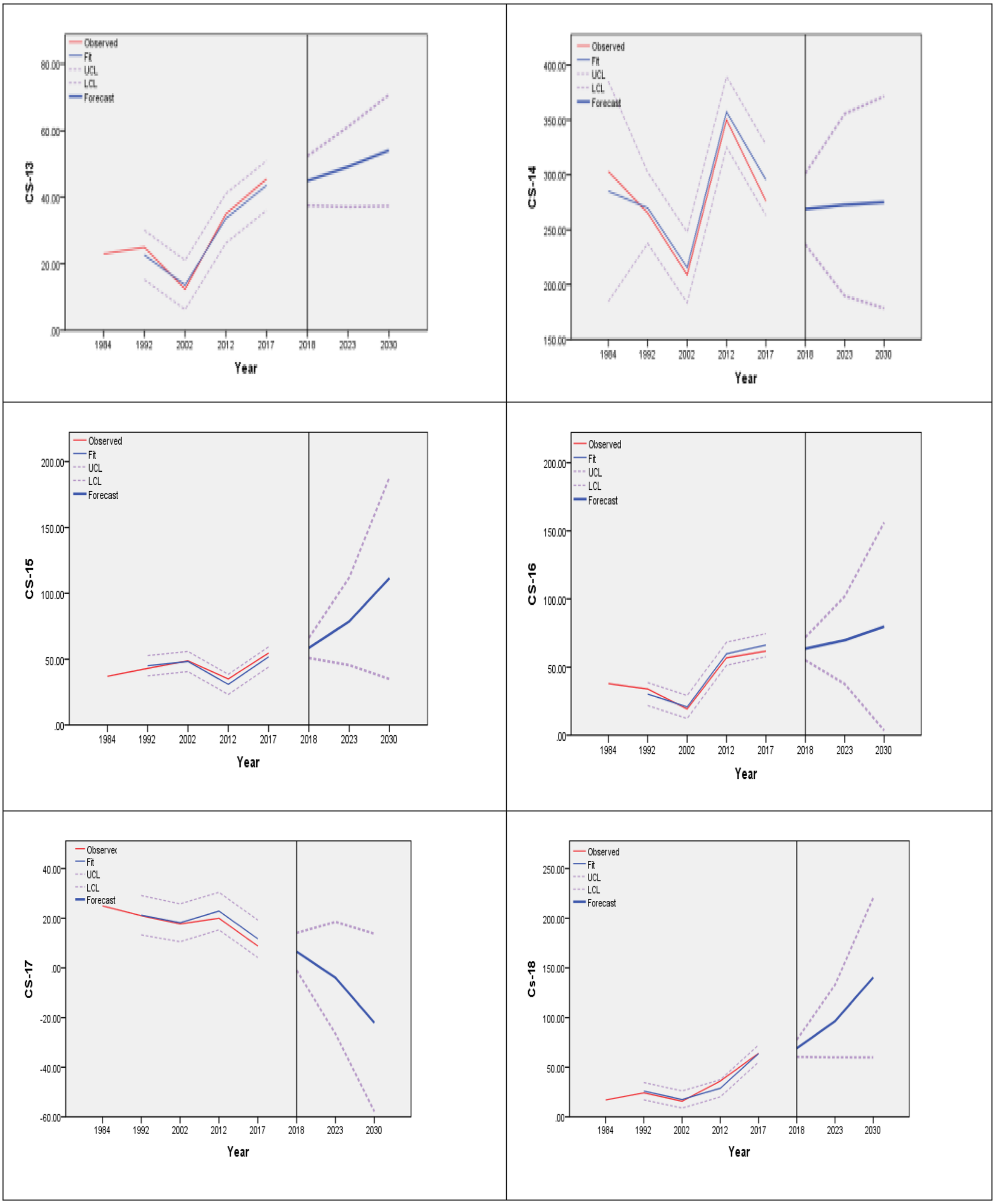

Fig. 13 continued.

centerline shifting rate (130.26 m/year) was observed at CS-6 under Satkarakandi part-1, whereas minimum centerline shifting rate (0.62 m/year) was found at CS-12 (Fig. 14). During different time intervals (1984–1992, 1984–2002, 1984–2012, 1984–2017), maximum shifting rate of centerline channel in the right bank was 130.26, 15.66, 101.80, and 85.72 m/year and

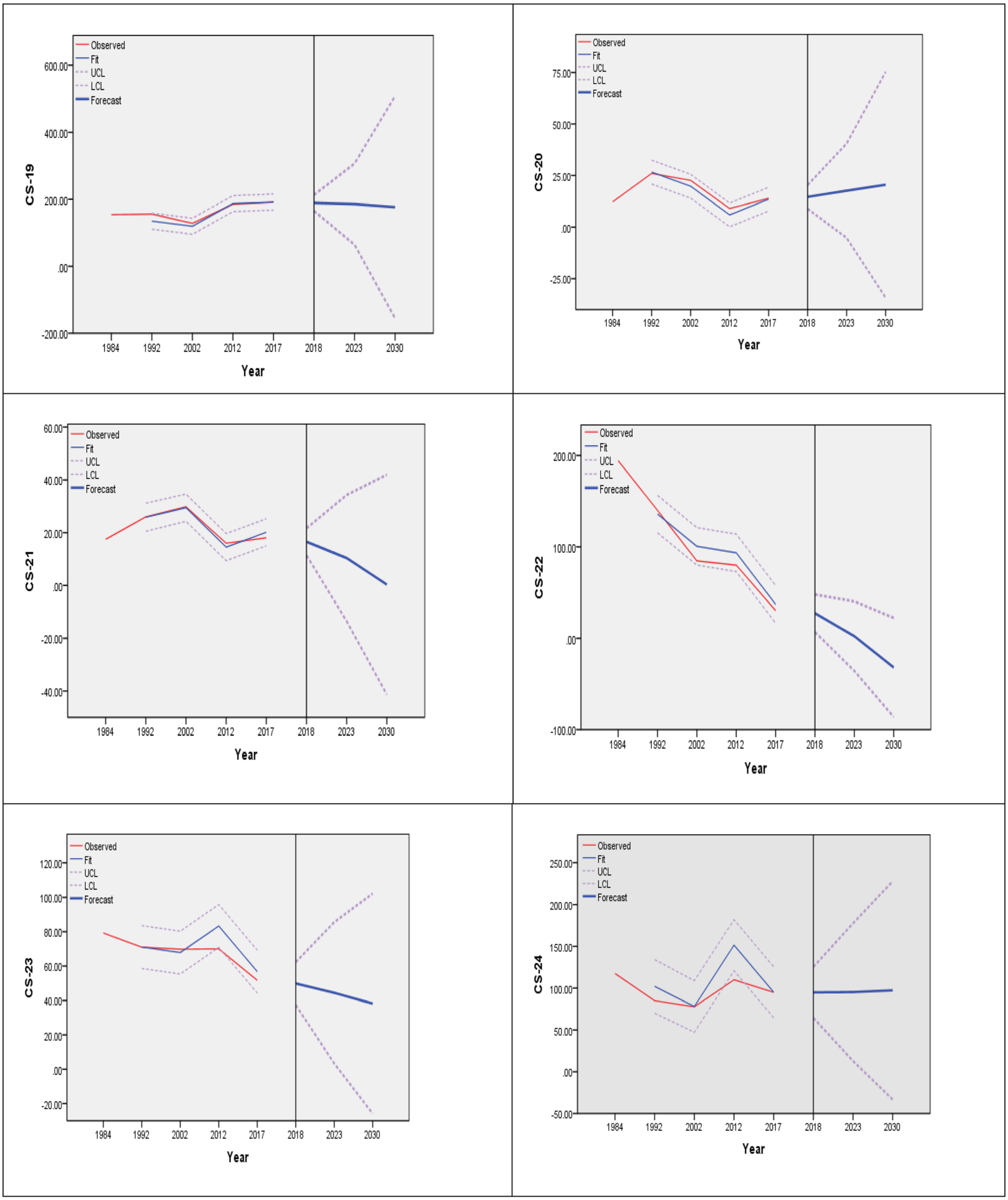

Fig. 13 continued.

maximum centerline channel shifting in the left bank was 47.53, 130.26, 38.43, and 33.10 m/year respectively (Table 4). In the right or left side of the river, shifting of river is evident; thus, the migration is noticeable in the river. From Fig. 14, it is found that certain cross-section (CS-5–7, CS-9–11, and CS-33–35) has some larger channel shifting. In a river system, river shifting

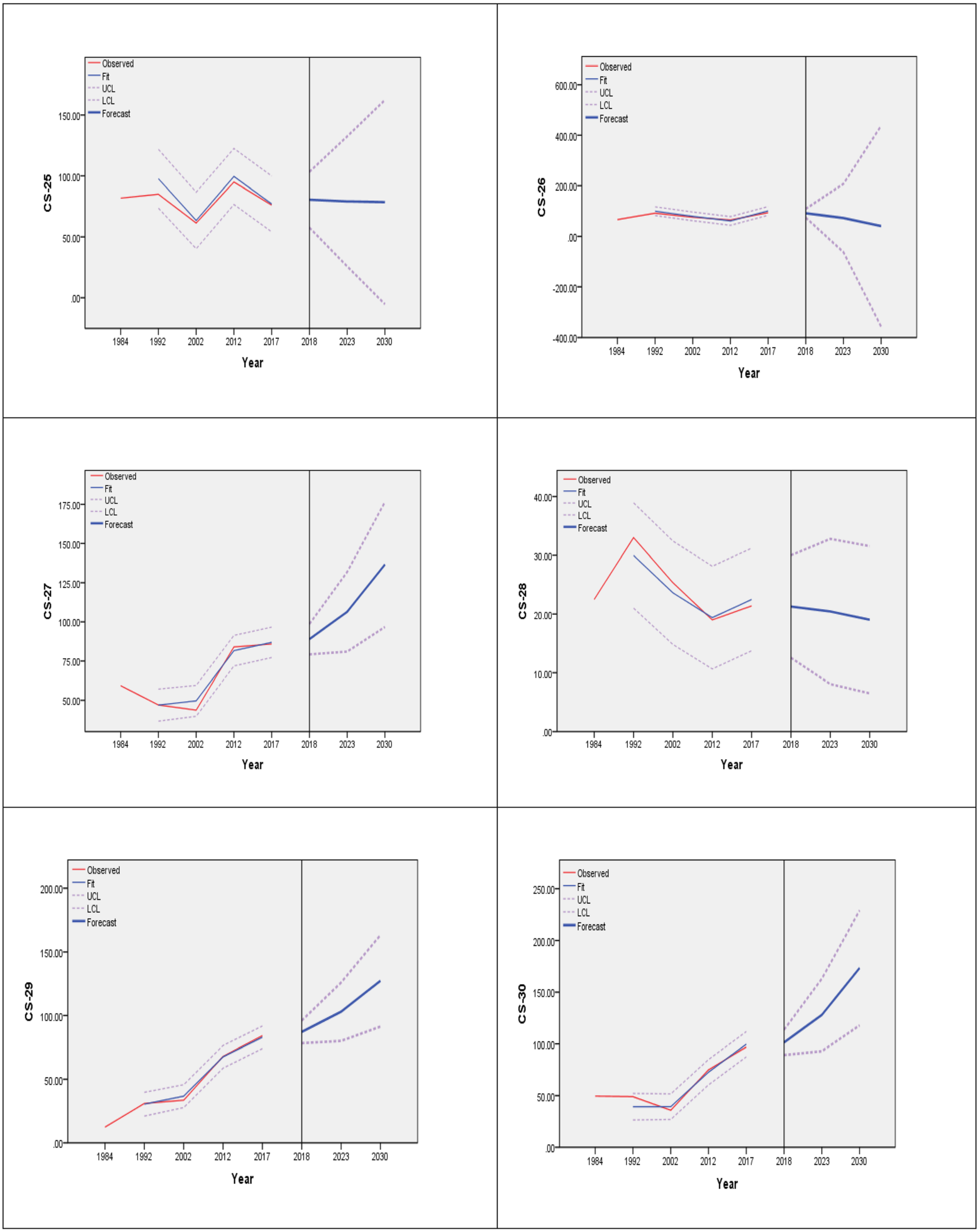

Fig. 13 continued.

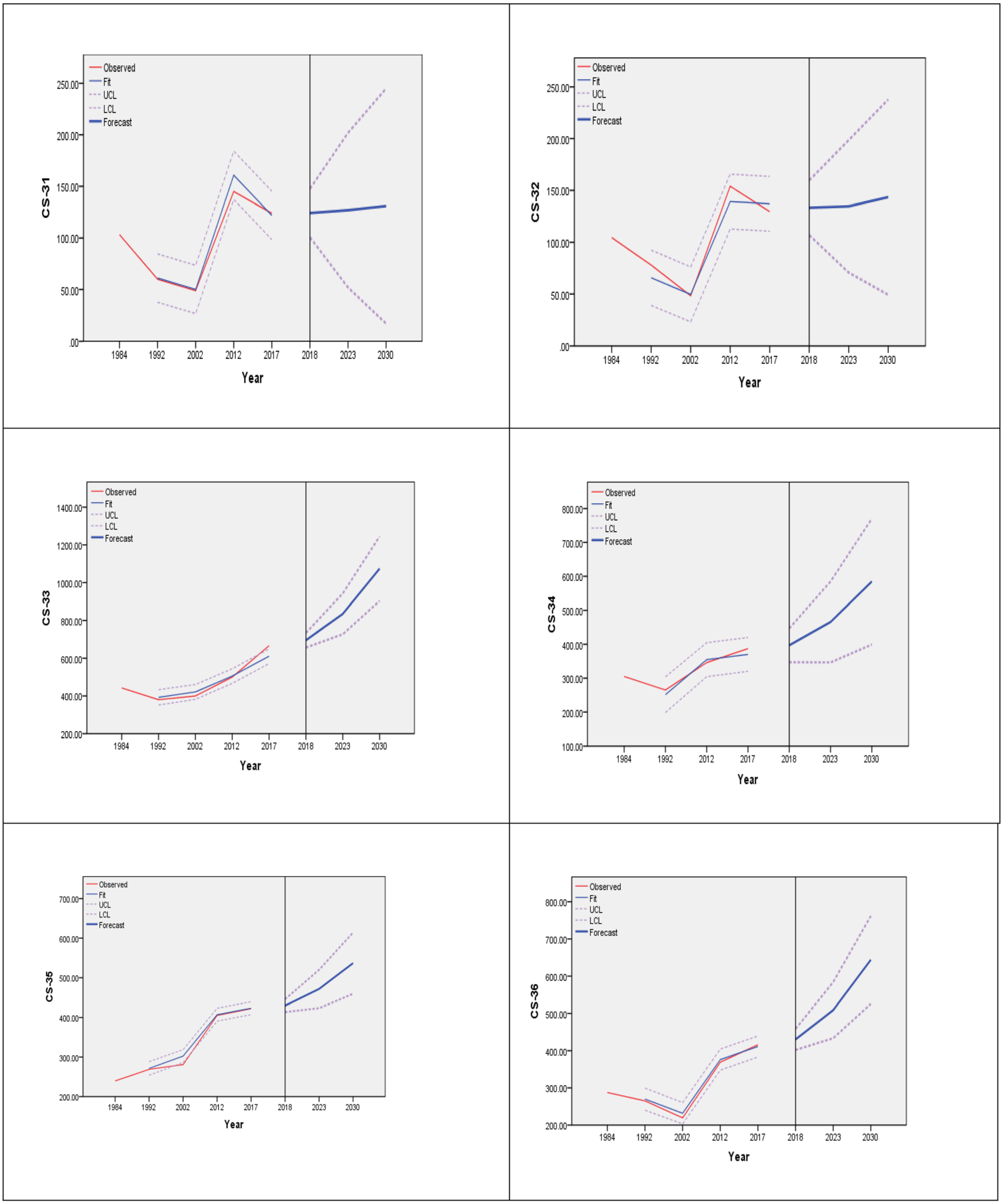

Fig. 13 continued.

may occur if the main channel of the river abruptly changes its course to a new river channel. Meandering rivers are especially vulnerable to such shifts. Wang et al. (2012) conducted a study in the alluvial reaches of the upper river considering the shift from 1950 to 2007 and found that up- and downshifts of the river banks are responsible for the long-term shifting rates of the

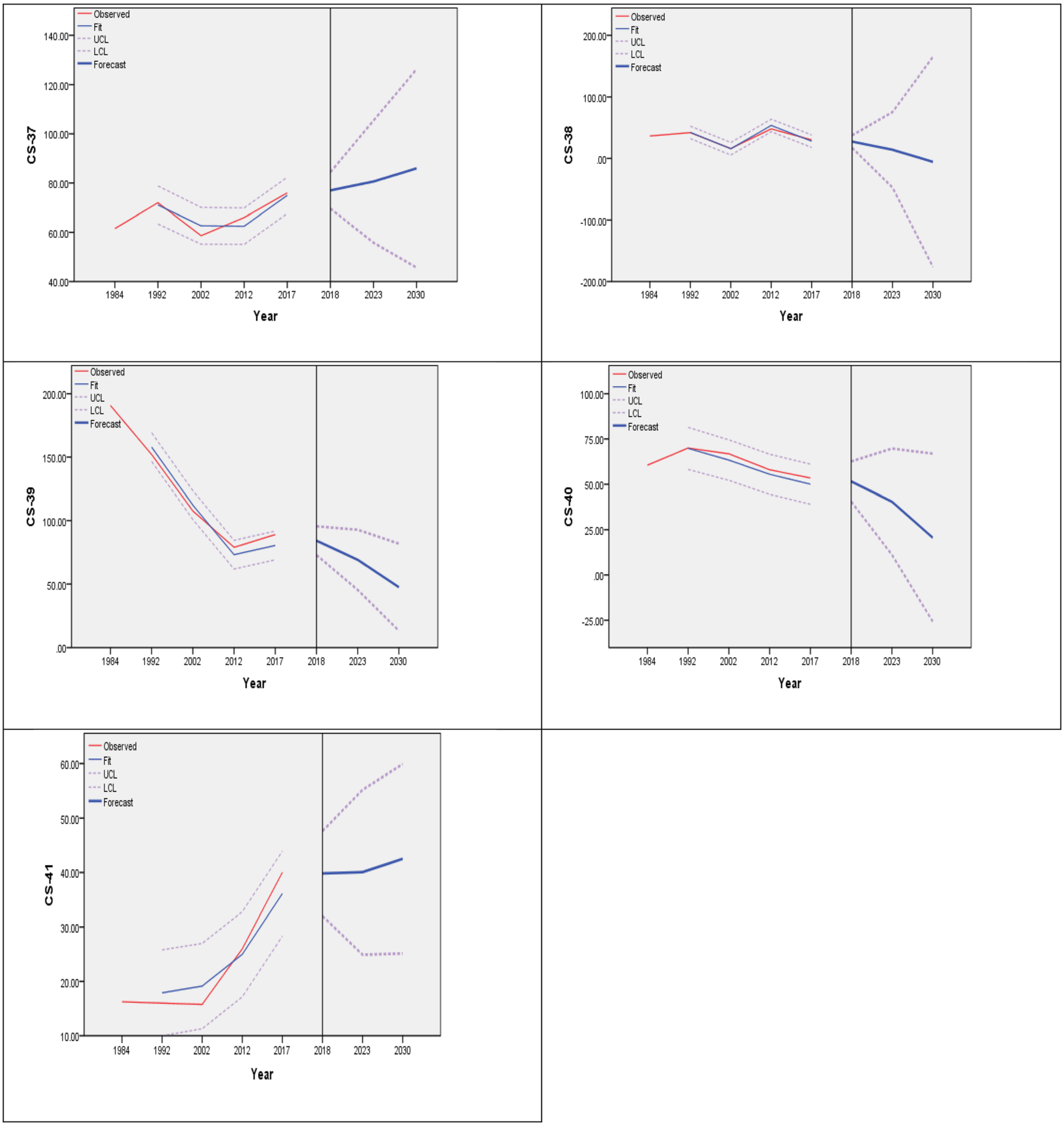

Fig. 13 continued.

channel. Bag et al. (2019) in the Bhagirathi River found that the actual shift of the channel usually follows a large flood event, but other factors make the system susceptible to the shift. Most commonly, sediment buildup blocks the river flow due to changes in current and riverbed gradient. In other cases, a cutoff occurs at the meandering neck in rivers with high channel sinuosity. Human activities such as farming, construction of houses, other temporary structures, and channel widening can also make the river system vulnerable to a sudden course change. A shift in river channel position has large impacts on the ecology, economy, and society, especially through impacts on water availability which is important for agriculture and transportation. Streamflow is mainly dependent on the rainfall, which give rise to annual flood periods (Gordon et al. 1992). More recurrent and prolonged heavy rains in the catchment result in flood regimes with damaging magnitude leading to river channel shifting rate in the river.

Means of channel migration rates for the right and left banks of the alluvial part of the Barak River in five different

Table 4 Lateral mid-line channel shifting rate (m/year) for each cross-section in the Barak River

Cross-section	1984–1992	1984–2002	1984–2012	1984–2017
CS-1	22.30 (R.B)	8.90 (R.B)	5.73 (R.B)	5.76 (R.B)
CS-2	20.66 (L.B)	9.05 (R.B)	5.18 (R.B)	4.76 (R.B)
CS-3	18.25 (R.B)	9.74 (L.B)	3.60 (L.B)	2.51 (L.B)
CS-4	15.28 (R.B)	6.53 (R.B)	4.65 (L.B)	3.79 (L.B)
CS-5	200.04 (R.B)	87.90 (L.B)	53.21 (R.B)	44.87 (R.B)
CS-6	297.27 (R.B)	130.26 (L.B)	101.80 (R.B)	85.72 (R.B)
CS-7	23.36 (R.B)	10.71 (R.B)	8.79 (R.B)	8.14 (R.B)
CS-8	2.45 (R.B)	1.27 (L.B)	1.62 (L.B)	1.76 (L.B)
CS-9	30.06 (L.B)	8.25 (L.B)	18.11 (L.B)	16.38 (L.B)
CS-10	132.75 (R.B)	58.23 (L.B)	38.43 (L.B)	33.10 (L.B)
CS-11	2.25 (R.B)	0.79 (R.B)	1.23 (L.B)	0.79 (L.B)
CS-12	2.12 (R.B)	0.62 (R.B)	0.34 (R.B)	0.18 (L.B)
CS-13	3.12 (R.B)	0.68 (R.B)	1.25 (L.B)	1.37 (R.B)
CS-14	33.13 (R.B)	11.66 (R.B)	11.43 (R.B)	8.36 (R.B)
CS-15	5.375 (R.B)	2.71 (R.B)	1.25 (R.B)	1.65 (R.B)
CS-16	4.25 (R.B)	1.07 (L.B)	2.04 (R.B)	1.87 (L.B)
CS-17	2.62 (L.B)	0.98 (R.B)	0.71 (L.B)	0.26 (L.B)
CS-18	3 (L.B)	0.87 (R.B)	1.30 (R.B)	1.93 (R.B)
CS-19	19.52 (R.B)	7.13 (R.B)	6.63 (R.B)	5.79 (R.B)
CS-20	3.27 (R.B)	1.25 (R.B)	0.32 (L.B)	0.42 (L.B)
CS-21	3.25 (R.B)	1.65 (R.B)	0.59 (R.B)	0.54 (L.B)
CS-22	17.54 (R.B)	4.81 (L.B)	2.87 (L.B)	0.92 (L.B)
CS-23	8.90 (R.B)	3.87 (L.B)	2.53 (L.B)	1.56 (L.B)
CS-24	10.65 (R.B)	4.31 (L.B)	3.94 (L.B)	2.87 (L.B)
CS-25	10.72 (R.B)	3.41 (L.B)	3.40 (L.B)	2.30 (L.B)
CS-26	11.53 (L.B)	4.21 (L.B)	2.34 (L.B)	2.84 (L.B)
CS-27	5.91 (R.B)	2.42 (L.B)	3.00 (L.B)	2.60 (L.B)
CS-28	4.18 (R.B)	1.40 (R.B)	0.71 (L.B)	0.64 (L.B)
CS-29	3.92 (R.B)	1.86 (L.B)	2.43 (L.B)	2.55 (L.B)
CS-30	6.19 (R.B)	1.96 (R.B)	2.70 (R.B)	2.93 (R.B)
CS-31	7.53 (R.B)	2.71 (L.B)	5.19 (L.B)	3.75 (L.B)
CS-32	9.82 (R.B)	2.68 (L.B)	5.52 (L.B)	3.92 (L.B)
CS-33	47.53 (L.B)	22.22 (R.B)	17.87 (R.B)	20.20 (R.B)
CS-34	33.23 (R.B)	18.09 (L.B)	12.39 (L.B)	11.73 (L.B)
CS-35	33.70 (R.B)	15.66 (R.B)	14.48 (R.B)	12.79 (R.B)
CS-36	33.20 (R.B)	12.18 (L.B)	13.20 (L.B)	12.61 (L.B)
CS-37	9.06 (R.B)	3.25 (L.B)	2.37 (L.B)	2.31 (L.B)
CS-38	5.31 (R.B)	0.89 (R.B)	1.71 (R.B)	0.91 (R.B)
CS-39	19.09 (R.B)	5.98 (R.B)	2.85 (R.B)	2.72 (L.B)
CS-40	8.81 (L.B)	3.71 (R.B)	2.09 (R.B)	1.61 (R.B)
CS-41	2.03 (R.B)	0.87 (R.B)	0.59 (L.B)	1.21 (L.B)

periods are shown in Table 5. Along the right bank, maximum average centerline channel shifting was identified in the period of 1984–1992, and the maximum average centerline channel shifting for the left bank was identified in the period of 1984–2002, while as along the right bank, minimum average centerline channel shifting was identified in the period of 1984–2002, and minimum average centerline channel shifting for the left bank was identified in the period of 1984–2017. Figure 15 shows the variation of mean of centerline channel shifting from various time periods. Along both the banks of the river (left bank and right bank), mean of centerline channel shifting is decreasing from 1984 to 2017. Limited information is available on the effects of earthquake shocks or plate tectonics in the upper and lower reaches of Barak River, and thus, their impact on river channel dynamics is a matter to be considered in future investigations as this may have some effect on centerline channel shifting and finally the river behavior.

Recommendations

In the present study, we have analyzed the morphometric parameters and temporal shifting of centerline channel shifting of the Barak River and give us the future synoptic view of the river course. During this study, various results and database are created, particularly the cross-sections, combined with the hydrographic data, and digital elevation model of floodplain can be further used for the hydraulic and sedimentation modeling which could make this study more interesting. Also river bank erosion/deposition risk map can be generated based on this modeling. Hence, this study can become very much helpful for future mitigation and hazard preparedness programs to be taken by the government authority.

Conclusion

The Barak River, flowing through the alluvial plains of Assam, experiences regular bank shifting and development of cutoffs posing threat to the habitants residing nearby. The main incentive of the present study is to understand the changes in river morphometric parameters and shifting of centerline channel shifting of the Barak River in order to understand the dynamics of channel. Five different years of Landsat images was used with ARIMA modeling in order to find the changes in the river for the 46 years (1984–2030). Our observation reveal that the morphological analysis indicates that sinuosity, wavelength, and radius of curvature from 1984 to 2017 show a decreasing trend. The sinuosity value in most of the meandering reaches is greater than 1.5. Results also show that all types of bend migration were observed to occur (extension, rotation, and translation). Formation of oxbow lake and neck cutoff was also found in reach-1 and reach-3 respectively. The outcome of ARIMA model specifies that channel shifting of centerline is going to change suddenly either to rightward or leftward directions. Throughout the whole alluvial part of the Barak River, rightward side is recognized as major concern. Results obtained from the analysis of channel shifting rates

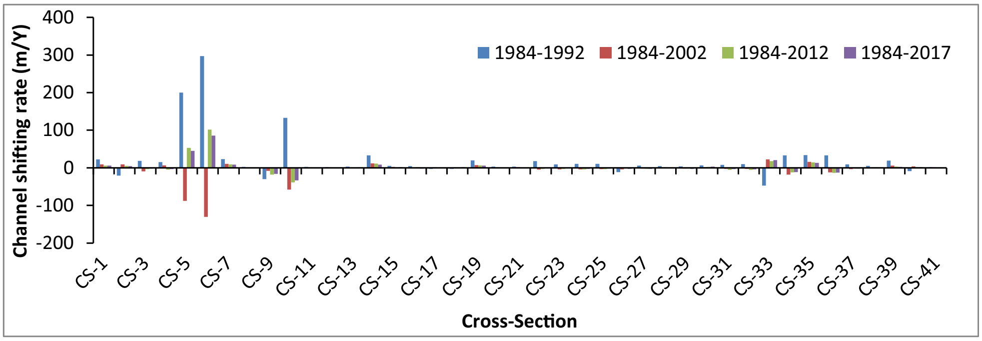

Fig. 14 Spatial lateral centerline channel shifting rate (m/year) for each cross-section in five different periods

Table 5 The mean channel shifting rate (m/year) of the Barak River

Direction	1984–1992		1984–2002		1984–2012		1984–2017	
	Number of CS	Rate	Number of CS	Rate	Number of CS	Rate	Number of CS	Rate
Rightward	34	29.67	22	5.28	18	13.33	15	13.09
Leftward	7	17.74	19	18.97	23	5.67	26	4.54
Mean	41	27.64	41	11.63	41	9.03	41	7.88

indicate that from 198 to 2017, maximum rate of centerline channel shifting in the right bank was 85.72 m/year at CS-6 and maximum rate of centerline channel shifting in the left bank was 33.10 m/year at CS-10. Moreover, results obtained from the centerline channel shifting, it can be said that in future period of time, Satkarakandi part-1 will be more vulnerable than Bhairabnagar. It is believed that the outcomes of this study shall form a base in understanding the future dynamics and bank migration of the alluvial rivers. We propose that future effects of bank migration may be prevented by adapting scientific bank protection measures and efficient planning of the adjacent settlements.

Acknowledgments We are thankful to USGS, CWC Shillong and other stack holders for providing us data, and other support for completion of this work.

Funding information We are thankful to DST-SERB, Govt. of India (ECR/2017/000344), for providing fund and support to carry out this research work.

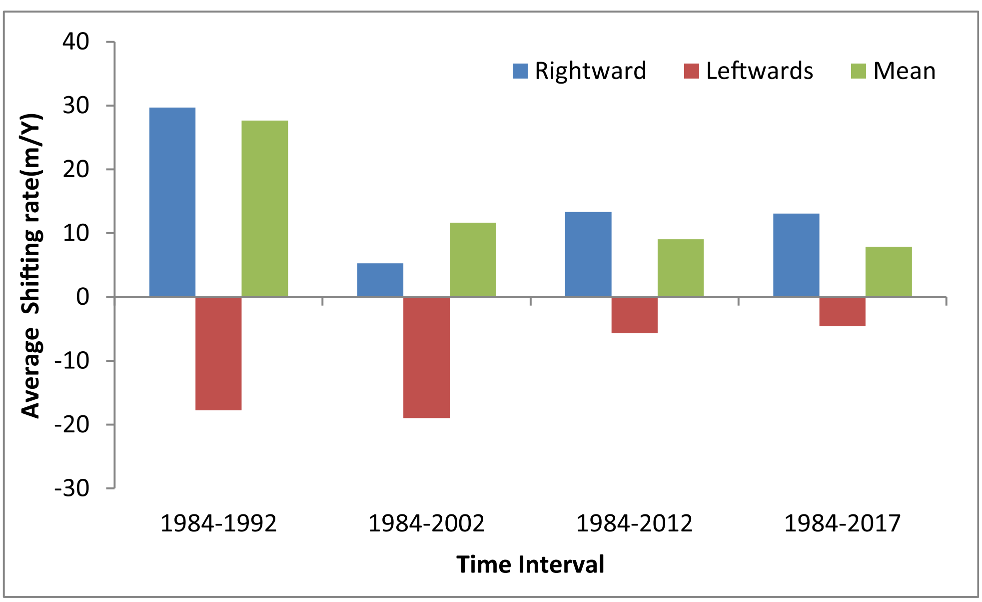

Fig. 15 Average centerline channel shifting rate (m/year) of the Barak River during five different periods

Compliance with ethical standards

Conflict of interest The authors declare that they have no conflict of interest.

References

Ahmed AA, Fawzi A (2011) Meandering and bank erosion of the River Nile and its environmental impact on the area between Sohag and El-Minia, Egypt. Arab J Geosci 4(1–2):1–11

Akhter S, Eibek KU, Islam S, Islam ARMT, Chu R, Shuanghe S (2019) Predicting spatiotemporal changes of channel morphology in the reach of Teesta River, Bangladesh using GIS and ARIMA modeling. Quat Int 513:80–94

Archana S, Garg RD, Nayan S (2012) RS-GIS based assessment of river dynamics of Brahmaputra River in India. J Water Resour Prot 2012

Bag R, Mondal I, Bandyopadhyay J (2019) Assessing the oscillation of channel geometry and meander migration cardinality of Bhagirathi River, West Bengal, India. J Geogr Sci 29(4):613–634

Box GEP and Jenkins GM (1970) Time series analysis; forecasting and control. Holden-Day, San Francisco (CA)

Brice James Coble (1982) Stream channel stability assessment. United States. Federal Highway Administration

Choudhury P, Ullah N (2014) Downstream flow top width prediction in a river system. Water SA 40(3):481–490

Chu ZX, Sun XG, Zhai SK, Xu KH (2006) Changing pattern of accretion/erosion of the modern Yellow River (Huanghe) Subaerial Delta, China: based on remote sensing images. Mar Geol 227(1–2):13–30

da Silva Ferreira, Maria Ana and Ebrahimi Mohsen (2017) “Meandering morphodynamics: insights from laboratory and numerical experiments and beyond”

Dar RA, Romshoo SA, Chandra R, Mir I (2014) Tectono geomorphic study of Karewa basin of Kashmir Himalayas. J Asian Earth Sci: 143–156

Das S (2018) Geomorphic characteristics of a Bedrock River inferred from drainage quantification, longitudinal profile, Knickzone identification and concavity analysis: a DEM-based study. Arab J Geosci 11(21):680

Das S, Pardeshi SD (2018) Morphometric analysis of Vaitarna and Ulhas River basins, Maharashtra, India: using geospatial techniques. Appl Water Sci 8(6):158

Das JD, Dutta T, Saraf AK (2007) Remote sensing and GIS application in change detection of the Barak River channel, NE India. J Indian Soc Remote Sens 35(4):301–312

De Rose RC, Basher LR (2011) Measurement of river bank and cliff erosion from sequential LIDAR and historical aerial photography. Geomorphology 126(1–2, 132):–47

Deb M, Ferreira C (2015) Planform Channel dynamics and Bank migration Hazard assessment of a highly Sinuous River in the north-eastern zone of Bangladesh. Environ Earth Sci 73(10):6613–6623

Deb S, Sil BS (2019) Climate change study for the meteorological variables in the Barak River basin in North-East India. Urban Clim 30: 100530

Debnath J, Pan ND, Ahmed I, Bhowmik M (2017) Channel migration and its impact on land use/land cover using RS and GIS: a study on Khowai River of Tripura, North-East India. Egypt J Remote Sens Space Sci 20(2):197–210

Dewan A, Corner R, Saleem A, Rahman MM, Haider MR, Rahman MM, Sarker MH (2017) Assessing channel changes of the Ganges-Padma River system in Bangladesh using Landsat and hydrological data. Geomorphology 276:257–279

Dhari S, Arya DS, Murumkar AR (2015) Application of remote sensing and GIS in sinuosity and river shifting analysis of the Ganges River in Uttarakhand Plains. Appl Geomatics 7(1):13–21

Djekovic V, Milosevic N, Andjelkovic A, Djurovic N, Barovic G, Vujacic D, Spalevic V (2016) Channel morphology changes in the river Pestan, Serbia. J Environ Prot Ecol 17(3):1203–1213

Engel FL, Rhoads BL (2012) Interaction among mean flow, turbulence, bed morphology, bank failures and channel planform in an evolving compound meander loop. Geomorphology 163:70–83

Evans P (1932) Tertiary succession in Assam. Trans Min Geol Inst India 27:155–260

Evans P (1964) Tectonic framework of Assam. J Geol Soc India 5:80–96

Fargue Louis (1867) Etude Sur La Corrélation Entre La Configuration Du Lit et La Profondeur d’eau Dans Les Rivières à Fond Mobile. Dunod

Friend PF, Sinha R (1993) Braiding and meandering parameters, vol. 75. Geological Soc London Special Pub, pp. 105–111

Gordon ND, McMahon TA, Finlayson BL (1992) Stream hydrology. An introduction for ecologists. Centre for Environmental Applied Hydrology. University of Melbourne. Wiley

Graf WL (2000) Locational probability for a dammed, urbanizing stream: Salt River, Arizona, USA. Environ Manag 25:321–335. https://doi.org/10.1007/s002679910025

Grove R, James JC, Thompson C (2013) Quantifying different riverbank erosion processes during an extreme flood event. Earth Surf Process Landf 38(12):1393–1406

Heitmuller FT, Hudson PF, Kesel RH (2017) Overbank sedimentation from the historic AD 2011 flood along the lower Mississippi River, USA. Geology 45(2):107–110

Henshaw AJ, Gurnell AM, Bertoldi W, Drake NA (2013) An assessment of the degree to which Landsat TM data can support the assessment of fluvial dynamics, as revealed by changes in vegetation extent and channel position, along a large river. Geomorphology 202:74–85

Heo J, Duc TA, Cho H-S, Choi S-U (2009) Characterization and prediction of meandering channel migration in the GIS environment: a case study of the Sabine River in the USA. Environ Monit Assess 152(1–4):155

Hooke JM (1980) Magnitude and distribution of rates of river bank erosion. Earth Surf Process 5(2):143–157

Howett Julia (2017) “Meander belt delineation: developing a predictive model for meander Belt width”

Hughes ML, McDowell PF, Andrew Marcus W (2006) Accuracy assessment of georectified aerial photographs: implications for measuring lateral channel movement in a GIS. Geomorphology 74(1–4):1–16

Inglis CC, Lacey G (1947) Meanders and their bearing on river training. maritime and waterways engineering division. Inst Civil Eng Eng Div Pap 5(17):3–24

Islam A, Guchhait SK (2017) Analysing the influence of Farakka Barrage Project on channel dynamics and meander geometry of Bhagirathi river of West Bengal, India. Arab J Geosci 10(11):245

Jain SK, Agarwal PK, Singh VP (2007) Hydrology and water resources of India, vol 57. Springer Science & Business Media

Jansen PPh, Van Bendegom L, Van Den Berg JH, de Vries MB, and Zanen A (1994) Principles of river engineering: the non-tidal alluvial river

Jaskuła J, Sojka M, Wicher-Dysarz J (2018) Analysis of the vegetation process in a two-stage reservoir on the basis of satellite imagery—a case study: Radzyny reservoir on the Sama river. Rocznik Ochrona Środowiska 20

Jefferson Mark (1902) Limiting width of meander belts. National Geographic Society

Keady DM and Priest MS (1977) “The downstream migration rate of river meandering patterns.” pp. 29–34 in Mississippi Water Resources Conference, Meeting 12th Mississippi Water Resources Conference, Jackson, MS.

Lawler DM (1993) The measurement of river bank erosion and lateral channel change: a review. Earth Surf Process Landf 18:777–821

Leopold Luna Bergere and Wolman Markley Gordon (1957) River channel patterns: braided, meandering, and straight. US Government Printing Office
Li Z, Yu G-A, Brierley GJ, Wang Z, Jia Y (2017) Migration and cutoff of meanders in the hyperarid environment of the middle Tarim River, northwestern China. Geomorphology 276:116–124
Magdaleno F, Fernández-Yuste JA (2011) Meander dynamics in a changing river corridor. Geomorphology 130(3–4):197–207
Magliulo P, Bozzi F, Pignone M (2016) Assessing the planform changes of the Tammaro River (southern Italy) from 1870 to 1955 using a GIS-aided historical map analysis. Environ Earth Sci 75(4):355
Milton EJ, Gilvear DJ, Hooper ID (1995) Investigating change in fluvial systems using remotely sensed data. In: Gurnell A, Petts G (eds) Changing river channels. Wiley, New York, pp 276–301
Mithun D, Dabojani D, Misbah U (2012) Evaluation of meandering characteristics using RS & GIS of Manu River. J Water Resour Prot 2012
Mount NJ, Tate NJ, Sarker MH, Thorne CR (2013) Evolutionary, multiscale analysis of river bank line retreat using continuous wavelet transforms: Jamuna River, Bangladesh. Geomorphology 183:82–95
Nandy DR, Das Gupta S, Sarkar K, Ganguly A (1983) Tectonic evolution of Tripura-Mizoram fold Belt, Surma Basin, Northeast India. Quart J Geol Min Met Soc India 55(4):186–194
Nanson GC, Hickin EJ (1983) Channel migration and incision on the Beatton River. J Hydraul Eng 109(3):327–337
Nanson GC, Hickin EJ (1986) A statistical analysis of bank erosion and channel migration in western Canada. Geol Soc Am Bull 97(4):497–504
Nawfee SM, Dewan A, Rashid T (2018) Integrating subsurface stratigraphic records with satellite images to investigate channel change and bar evolution: a case study of the Padma River, Bangladesh. Environ Earth Sci 77(3):89
Nicoll TJ, Hickin EJ (2010) Planform geometry and channel migration of confined meandering rivers on the Canadian prairies. Geomorphology 116(1–2):37–47
O'Boyle JM (1981) Relationships between the morphometric parameters of meander planform in south County Down. Ir Geogr 14(1):65–74
Ollero A (2010) Channel changes and floodplain management in the meandering middle Ebro River, Spain. Geomorphology 117(3–4): 247–260
Pati JK, Jyoti L, Prakash K, Bhusan R (2008) Spatio-temporal shift of western bank of the Ganga river, Allahabad city and its implications. J Indian Soc Remote Sens 36(3):289–297
Peixoto JMA, Nelson BW, Wittmann F (2009) Spatial and temporal dynamics of river channel migration and vegetation in central Amazonian white-water floodplains by remote-sensing techniques. Remote Sens Environ 113(10):2258–2266
Pourbakhshian S, Pouraminian M (2015) Stochastic modeling to prediction of river morphological changes. Indian J Sci Technol 8(12):1
Raju ATR (1968) Geological evolution of Assam and Cambay Tertiary basins of India. Bull Am Assoc Pet Geol 52(12):2422–2437
Roca M, Martín-Vide JP, Blanckaert K (2007) Reduction of bend scour by an outer bank footing: footing design and bed topography. J Hydraul Eng 133(2):139–147
Schumm SA (1973) Geomorphic thresholds and complex response of drainage systems. Fluvial Geomorphol 6:69–85
Seshavataram BTV, Nandi PK and Choudhury S (1998) Petroleum geology of Cachar fold belt, Proc. Reg. Sem. Dev. Geol. Res. in N.E. India, Gauhati University, pp.327–348
Tangri AK (2000) Application of remote sensing techniques in monitoring the spatial and temporal evolution of fluvio-geomorphic features in Ganga basin with specific reference to their impact on engineering structures. In Sinha R (ed) Proceedings of the workshop on Fluvial geomorphology with special reference to floodplains. Indian Institute of Technology, Kanpur
Thakur PK, Laha C, Aggarwal SP (2012) River bank erosion hazard study of river Ganga, upstream of Farakka Barrage using remote sensing and GIS. Nat Hazards 61(3):967–987
Timár G (2003) Controls on channel sinuosity changes: a case study of the Tisza River, the Great Hungarian Plain. Quat Sci Rev 22(20): 2199–2207
Wang S, Yan Y, Li Y (2012) Spatial and temporal variations of suspended sediment deposition in the alluvial reach of the upper Yellow River from 1952 to 2007. Catena 92:30–37. https://doi.org/10.1016/j.catena.2011.11.012
Wellmeyer JL, Slattery MC, Phillips JD (2005) Quantifying downstream impacts of impoundment on flow regime and channel planform, lower Trinity River, Texas. Geomorphology 69(1–4):1–13
Williams GP (1986) River meanders and channel size. J Hydrol 88(1–2): 147–164
Xia J, Deng S, Lu J, Xu Q, Zong Q, Tan G (2016) Dynamic channel adjustments in the Jingjiang Reach of the Middle Yangtze River. Sci Rep 6:22802
Yang X, Damen MCJ, Van Zuidam RA (1999) Satellite remote sensing and GIS for the analysis of channel migration changes in the active Yellow River Delta, China. Int J Appl Earth Obs Geoinf 1(2):146–157
Yousefi S, Pourghasemi HR, Hooke J, Navratil O, Kidová A (2016) Changes in morphometric meander parameters identified on the Karoon River, Iran, using remote sensing data. Geomorphology 271:55–64
Yousefi S, Moradi HR, Pourghasemi HR, Khatami R (2017) Assessment of floodplain landuse and channel morphology within meandering reach of the Talar River in Iran using GIS and aerial photographs. Geocarto Int:1–14
Zaimes GN, Schultz RC, Isenhart TM (2004) Stream bank erosion adjacent to riparian forest buffers, row-crop fields, and continuously-grazed pastures along Bear Creek in central Iowa. J Soil Water Conserv 59(1):19–27
Zolezzi G, Luchi R, Tubino M (2012) Modeling morphodynamic processes in meandering rivers with spatial width variations. Rev Geophys 50(4)